



國立臺灣大學工學院化學工程學系

碩士論文

Department of Chemical Engineering

College of Engineering

National Taiwan University

Master's Thesis

帶電軟質粒子在表面帶電孔洞中之沉降運動

Sedimentation of a Charged Soft Particle in a Charged

Cavity

林永捷

Yong-Jie Lin

指導教授：葛煥彰 教授

Advisor: Huan-Jang Keh, Professor

中華民國 一百一十三 年 七 月

July, 2024

國立臺灣大學碩士學位論文
口試委員會審定書

帶電軟質粒子在表面帶電孔洞中之沉降運動
Sedimentation of a Charged Soft Particle in a Charged
Cavity

本論文係林永捷君（R11524103）在國立臺灣大學化學工程學系
所完成之碩士學位論文，於民國一百一十三年七月五日承下列考試委
員審查通過及口試及格，特此證明

口試委員：

萬煥朝

(簽名)

詹正雄

(指導教授)

謝工璽

系主任、所長

廖英志

(簽名)

謝辭



在這篇論文完成的時刻，我想要衷心地感謝所有在這段學術旅程中給予我支持和鼓勵的人們。首先，我要感謝我的指導教授葛煥彰教授，您的悉心指導和寶貴建議是我完成這篇論文的重要支柱。感謝您在整個研究過程中給予我的專業指導和深刻啟發，您的教導對我的學術成長至關重要。

同時，我也要感謝口試委員們，感謝您們抽出寶貴的時間閱讀並提出寶貴的意見和建議。這些寶貴的反饋幫助我不斷改進論文的品質，使其更加完善。

除此之外，我要深深地感謝我的家人和朋友。感謝你們在我學術生涯中給予的無限支持和理解，無論是情感上的支持還是物質上的幫助，都是我不斷前行的動力源泉。

最後，我也要感謝所有在我學習過程中給予過幫助的實驗室同學們。與你們的討論和交流激發了我的思維，使我在學術道路上不斷進步。這篇論文的完成不僅代表了我的努力和成果，更是各位在我學術旅程中無私支持和鼓勵的結果。在此，我衷心地向各位表達最誠摯的謝意和深深的感激。

摘要



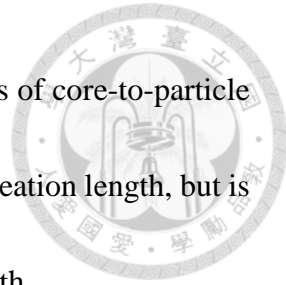
本文探討一個球形軟質粒子在一個充滿對稱電解質溶液的球形孔洞內之沉降運動，軟質粒子由一個未帶電的球形硬核和一個包覆在外帶電的均勻多孔層組成。在假設系統些微偏離平衡狀態的情況下，利用常規微擾法，以多孔層的空間電荷密度和孔洞的表面電荷密度為微小參數，將主導流場、電位和電化學位能分布的非線性的電動力方程式簡化成為線性化方程式，並結合適當的邊界條件，求解了線性化電動力方程式後，再利用重力、流體阻力和電力的合力平衡，求解出軟質粒子沉降速度的表示式。本研究發現孔洞表面帶電可以增加軟質粒子的沉降速度，主要是由於沉降電位梯度造成的孔洞內電滲透使流體循環流動加強。除此之外，多孔層中的空間電荷和孔洞表面電荷電性相同時，粒子速度大致上會因孔洞的影響而增加。當此二固定電荷電性相反時，孔洞表面電荷密度相對於多孔層空間電荷密度足夠多時，則會增加粒子速度。孔洞表面電荷對軟質粒子沉降速度的影響會因為硬核與粒子半徑比、粒子與孔洞半徑比和粒子半徑與流體於多孔層內滲透長度的比值減小而增加，但此影響不是粒子半徑與電雙層厚度的比值的單調變化函數。

關鍵詞：沉降速度；帶電軟質粒子；帶電孔洞；電動力學；邊界效應

Abstract



The sedimentation of a soft particle composed of an uncharged hard sphere core and a charged porous surface layer inside a concentric charged spherical cavity full of a symmetric electrolyte solution is analyzed in quasi-steady state. By using a regular perturbation method with small fixed charge densities of the soft sphere and cavity wall, a set of linearized electrokinetic equations relevant to the fluid velocity field, electrical potential profile, and ionic electrochemical potential energy distributions are solved. A closed-form formula for the sedimentation velocity of the soft sphere is obtained as a function of the ratios of core-to-particle radii, particle-to-cavity radii, particle radius to the Debye screening length, and particle radius to porous layer permeation length. The existence of the surface charge on the cavity wall increases the settling velocity of the charged soft sphere, principally because of the electroosmotic enhancement of fluid recirculation within the cavity induced by the sedimentation potential gradient. When the porous layer space charge and cavity wall surface charge have the same sign, the particle velocity is generally enhanced by the presence of the cavity. When these fixed charges have opposite signs, the particle velocity will be enhanced/reduced by the presence of the cavity if the wall surface charge density is sufficiently large/small relative to the porous layer space charge density in magnitude. The effect of the wall surface charge on the



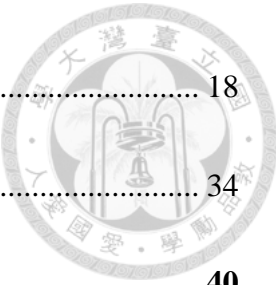
sedimentation of the soft sphere increases with decreases in the ratios of core-to-particle radii, particle-to-cavity radii, and particle radius to porous layer permeation length, but is not a monotonic function of the ratio of particle radius to Debye length.

Keywords: sedimentation velocity; charged soft particle; charged cavity; electrokinetics; boundary effect



Table of Contents

論文口試委員審定書	i
謝辭	ii
摘要	iii
Abstract	iv
Table of Contents	vi
List of Figures	viii
Chapter 1 Introduction	1
Chapter 2 Electrokinetic Equations.....	4
2.1. Differential Equations.....	6
2.2. Boundary Conditions.....	8
Chapter 3 Solution of Electrokinetic Equations	9
3.1. Equilibrium Electric Potential	9
3.2. Small Perturbations	11
3.3. Forces on the Particle	13
3.4. Sedimentation Velocity.....	15
Chapter 4 Results and Discussion	18



4.1. The Coefficient H_1 , H_2 , and H_3	18
4.2. The Normalized Sedimentation Velocity	34
Chapter 5 Conclusions	40
Notation	42
References.....	46
Appendix A Some Functions in Equations (15)-(17)	52

List of Figures



Figure 1. Geometric sketch for the sedimentation of a charged soft particle at the center

of a charged cavity. 5

Figure 2a. Plots of the coefficient H_1 in Eq. (26) for the sedimentation of a soft particle

in a cavity full of aqueous KCl solution versus the parameter κa with various

values of λa at $r_0/a = 0$ and $a/b = 0.5$ 22

Figure 2b. Plots of the coefficient H_1 in Eq. (26) for the sedimentation of a soft particle

in a cavity full of aqueous KCl solution versus the parameter a/b with

various values of κa at $r_0/a = 0$ and $\lambda a = 1$ 23

Figure 2c. Plots of the coefficient H_1 in Eq. (26) for the sedimentation of a soft particle

in a cavity full of aqueous KCl solution versus the parameter λa with various

values of r_0/a at $\kappa a = 1$ and $a/b = 0.5$ 24

Figure 2d. Plots of the coefficient H_1 in Eq. (26) for the sedimentation of a soft particle

in a cavity full of aqueous KCl solution versus the parameter r_0/a with

various values of a/b at $\kappa a = 1$ and $\lambda a = 1$ 25

Figure 3a. Plots of the coefficient H_2 in Eq. (26) for the sedimentation of a soft particle

in a cavity full of aqueous KCl solution versus the parameter κa with various

values of λa at $r_0/a = 0$ and $a/b = 0.5$ 26

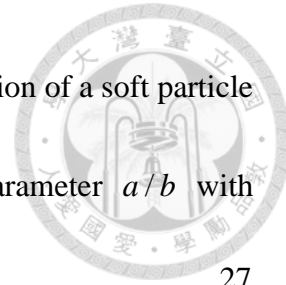


Figure 3b. Plots of the coefficient H_2 in Eq. (26) for the sedimentation of a soft particle in a cavity full of aqueous KCl solution versus the parameter a/b with various values of κa at $r_0/a = 0$ and $\lambda a = 1$ 27

Figure 3c. Plots of the coefficient H_2 in Eq. (26) for the sedimentation of a soft particle in a cavity full of aqueous KCl solution versus the parameter λa with various values of r_0/a at $\kappa a = 1$ and $a/b = 0.5$ 28

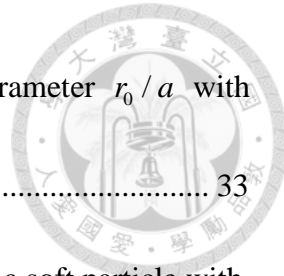
Figure 3d. Plots of the coefficient H_2 in Eq. (26) for the sedimentation of a soft particle in a cavity full of aqueous KCl solution versus the parameter r_0/a with various values of a/b at $\kappa a = 1$ and $\lambda a = 1$ 29

Figure 4a. Plots of the coefficient H_3 in Eq. (26) for the sedimentation of a soft particle in a cavity full of aqueous KCl solution versus the parameter κa with various values of λa at $r_0/a = 0$ and $a/b = 0.5$ 30

Figure 4b. Plots of the coefficient H_3 in Eq. (26) for the sedimentation of a soft particle in a cavity full of aqueous KCl solution versus the parameter a/b with various values of κa at $r_0/a = 0$ and $\lambda a = 1$ 31

Figure 4c. Plots of the coefficient H_3 in Eq. (26) for the sedimentation of a soft particle in a cavity full of aqueous KCl solution versus the parameter λa with various values of r_0/a at $\kappa a = 1$ and $a/b = 0.5$ 32

Figure 4d. Plots of the coefficient H_3 in Eq. (26) for the sedimentation of a soft particle



in a cavity full of aqueous KCl solution versus the parameter r_0/a with various values of a/b at $\kappa a = 1$ and $\lambda a = 1$ 33

Figure 5a. Plots of the normalized sedimentation velocity U/U_{00} of a soft particle with $\bar{Q}=1$ in a cavity full of aqueous KCl solution with $r_0/a = 0.5$, $\lambda a = 1$, and $\kappa a = 1$ versus the parameter $\bar{\sigma}$ for various values of a/b 36

Figure 5b. Plots of the normalized sedimentation velocity U/U_{00} of a soft particle with $\bar{Q}=1$ in a cavity full of aqueous KCl solution with $r_0/a = 0.5$, $a/b = 0.5$, and $\lambda a = 1$ versus the parameter $\bar{\sigma}$ for various values of κa 37

Figure 5c. Plots of the normalized sedimentation velocity U/U_{00} of a soft particle with $\bar{Q}=1$ in a cavity full of aqueous KCl solution with $r_0/a = 0.5$, $a/b = 0.5$, and $\kappa a = 1$ versus the parameter $\bar{\sigma}$ for various values of λa 38

Figure 5d. Plots of the normalized sedimentation velocity U/U_{00} of a soft particle with $\bar{Q}=1$ in a cavity full of aqueous KCl solution with $a/b = 0.5$, $\lambda a = 1$, and $\kappa a = 1$ versus the parameter $\bar{\sigma}$ for various values of r_0/a 39

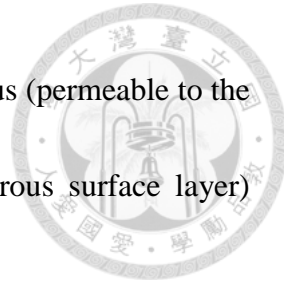
Chapter 1

Introduction



The sedimentation of charged particles in ionic fluids under gravity is a common phenomenon in various fields of colloidal science as well as biomedical, mechanical, chemical, civil, and environmental engineering [1,2]. This phenomenon is more complex than the migration of uncharged particles because the ambient fluid flow distorts the electrical double layer surrounding each charged particle and induces a sedimentation potential gradient [3,4]. This induced electric field alters the velocity distribution of the ionic fluid via the electrostatic interaction and diminishes the settling velocity of the charged particle by an electrophoretic effect.

Using a regular perturbation method, Booth [5] first obtained analytical formulas for the sedimentation velocity and potential in suspensions of hard (impermeable to the ionic fluid) spheres with arbitrary double layer thickness as power expansions in their low zeta potential. Numerical results relaxing the assumption of low zeta potential in this analysis was calculated by Stigter [6]. Ohshima et al. [7] obtained analytical formulas and numerical results of the sedimentation velocity and potential in suspensions of hard spheres for a wide range of zeta potential and double layer thickness. On the other hand, the regular perturbation analyses have been extended to obtain the sedimentation velocity



and potential in suspensions of interacting hard spheres [8-12], porous (permeable to the ionic fluid) spheres [13,14], and soft (hard core covered with porous surface layer) spheres [15,16].

In various applications of sedimentation, colloid particles are rarely unbounded but often settle close to solid boundaries [17,18]. In the past, the boundary effect on sedimentation of uncharged particles were studied extensively [19-23], but not much information of this effect on charged particles was conveyed. Pujar and Zydny [24] calculated the settling velocity of a charged spherical particle in a concentric uncharged spherical cavity using perturbation expansions of small zeta potentials and Peclet number. This thesis has been extended to numerical calculations in the case of arbitrary zeta potentials [25]. More recently, the settling of a charged hard [26] or porous [27] spherical particle within a con-centric charged spherical cavity with arbitrary electric double layers has been analytically investigated for the case of small fixed charge densities of the particle and cavity wall.

In this thesis, the sedimentation of a charged soft spherical particle inside a concentric charged spherical cavity with arbitrary double layer thickness is analytically studied. The fluid velocity, electric potential, and ionic electrochemical potential energy distributions satisfying the linearized electrokinetic equations are determined as power series of the small fixed charge densities of the soft sphere and cavity wall. A closed-form



formula for the settling velocity of the soft sphere is obtained as a function of relevant parameters.

Chapter 2

Electrokinetic Equations



As illustrated in Figure 1, we consider the quasi-steady sedimentation of a soft sphere of radius a , consisting of an uncharged hard sphere core of radius r_0 and a charged porous surface layer of thickness $a - r_0$, inside a concentric charged spherical cavity of radius b full of the fluid solution of a symmetric electrolyte. The porous surface layer is permeable to the electrolyte solution and has fixed charges distributed at a uniform space density. The gravitational acceleration field $g\mathbf{e}_z$ (\mathbf{e}_z is the unit vector in the z direction) is acting on the system and the sedimentation velocity $U\mathbf{e}_z$ of the soft sphere will be determined. The origin of the spherical coordinates (r, θ, φ) is attached to the particle/cavity center (at $z = 0$), and the system is independent of φ (symmetric about the z axis).

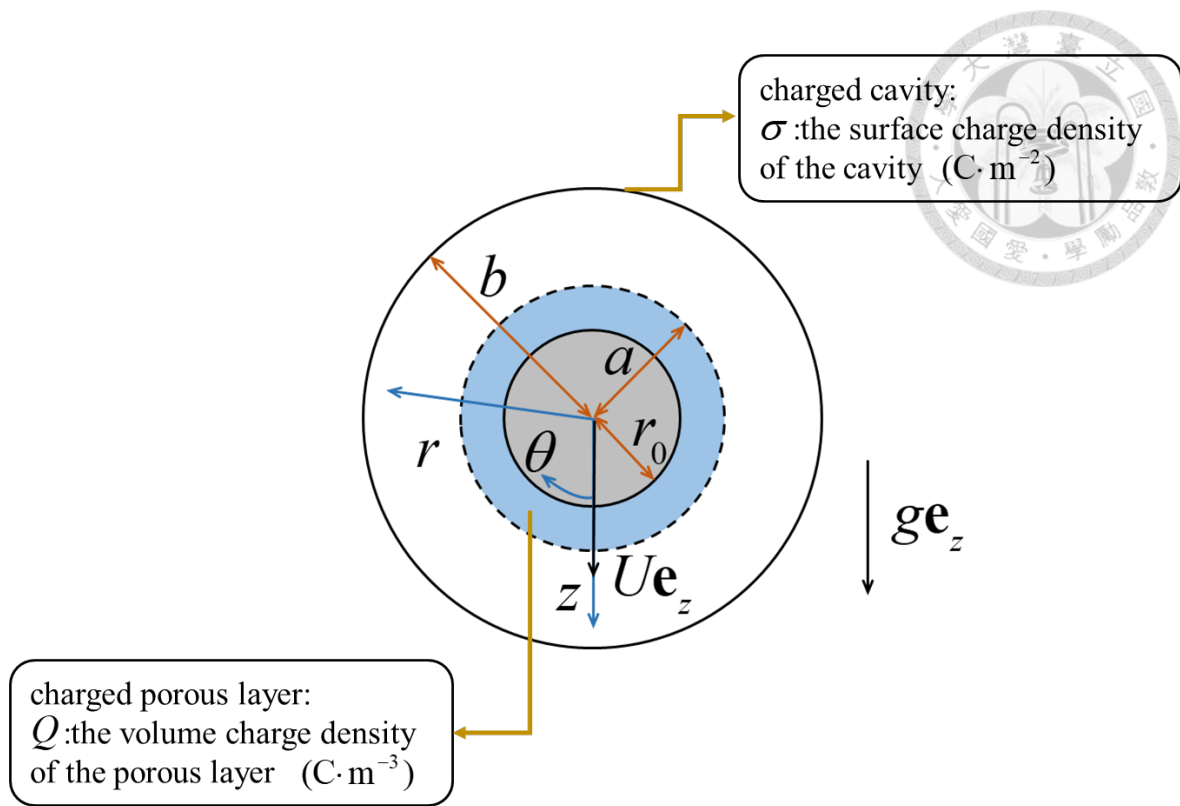


Figure 1. Geometric sketch for the sedimentation of a charged soft particle at the center

of a charged cavity.



2.1. Differential Equations

The system is assumed to deviate slightly from equilibrium. Therefore, the pressure profile $p(r, \theta)$, electrical potential field $\psi(r, \theta)$, and ionic concentration distributions $n_+(r, \theta)$ and $n_-(r, \theta)$ can be decomposed into

$$p = p^{(eq)} + \delta p, \quad (1a)$$

$$\psi = \psi^{(eq)} + \delta\psi, \quad (1b)$$

$$n_{\pm} = n_{\pm}^{(eq)} + \delta n_{\pm}, \quad (1c)$$

respectively, where $p^{(eq)}(r, \theta)$, $\psi^{(eq)}(r)$, and $n_{\pm}^{(eq)}(r)$ are the equilibrium pressure, electrical potential, and ionic concentrations, respectively [$n_{\pm}^{(eq)}(r)$ and $\psi^{(eq)}(r)$ are related by the Boltzmann equation], $\delta p(r, \theta)$, $\delta\psi(r, \theta)$, and $\delta n_{\pm}(r, \theta)$ are the small perturbed quantities to the relevant equilibrium fields, and the subscripts + and – denote the cation and anion, respectively.

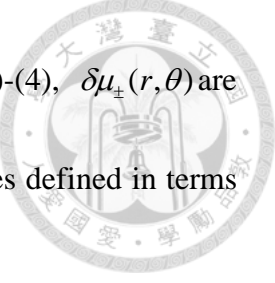
The small perturbations δp , $\delta\psi$, δn_{\pm} , and fluid velocity field $\mathbf{u}(r, \theta)$ satisfy the continuity equation of the incompressible fluid ($\nabla \cdot \mathbf{u} = 0$) and following linearized electrokinetic equations [13]:

$$\eta[\nabla^2 - h(r)\lambda^2]\mathbf{u} = \nabla\delta p - \varepsilon[\nabla^2\psi^{(eq)}\nabla\delta\psi + \nabla^2\delta\psi\nabla\psi^{(eq)}] - h(r)Q\nabla\delta\psi, \quad (2)$$

$$\nabla^2\delta\psi = \frac{Zen^\infty}{\varepsilon kT} [\exp(\frac{Zen\psi^{(eq)}}{kT})(\delta\mu_- + Ze\delta\psi) - \exp(-\frac{Zen\psi^{(eq)}}{kT})(\delta\mu_+ - Ze\delta\psi)], \quad (3)$$

$$\nabla^2\delta\mu_{\pm} = \pm\frac{Ze}{kT}\{\nabla\psi^{(eq)} \cdot \nabla\delta\mu_{\pm} - \frac{kT}{D_{\pm}}\nabla\psi^{(eq)} \cdot \mathbf{u}\}, \quad (4)$$

resulting from the modified Stokes/Brinkman equation, Poisson's equation, and



continuity equations of the ionic species, respectively. In Equations (2)-(4), $\delta\mu_{\pm}(r, \theta)$ are the perturbed quantities of the ionic electrochemical potential energies defined in terms of $\delta\psi$ and δn_{\pm} ,

$$\delta\mu_{\pm} = \pm Ze\delta\psi + \frac{kT}{n_{\pm}^{(\text{eq})}} \delta n_{\pm}, \quad (5)$$

η and ε are the viscosity and dielectric permittivity of the fluid, respectively, n° and Z are the bulk concentration and valence, respectively, of the symmetric electrolyte, D_{\pm} are the diffusivities of the ionic species, $1/\lambda$ is the square root of the permeability of the fluid in the porous surface layer of the soft sphere, $h(r)$ equals unity if $r_0 \leq r \leq a$ and zero otherwise, k is Boltzmann's constant, T is absolute temperature, and e is the charge of a proton.

For porous particles made of plastic foam slab [28] and steel wool [29], experimental data for $1/\lambda$ can be 400 microns, while in the surface layers of grafted polymer microcapsules [30], rat lymphocytes [31], and human erythrocytes [32] in electrolyte solutions, $1/\lambda$ was found as low as 3 nm.



2.2. Boundary Conditions

The boundary conditions of the perturbations \mathbf{u} , $\delta\psi$, and $\delta\mu_{\pm}$ at the interface between the hard sphere core and the porous surface layer and at the particle surface are

[15,33,34]

$$r = r_0 : \quad \mathbf{u} = \mathbf{0}, \quad \mathbf{e}_r \cdot \nabla \delta\psi = 0, \quad \mathbf{e}_r \cdot \nabla \delta\mu_{\pm} = 0, \quad (6)$$

$$r = a : \quad \mathbf{u}, \quad \mathbf{e}_r \cdot \boldsymbol{\tau}, \quad \delta\psi, \quad \nabla \delta\psi, \quad \delta\mu_{\pm}, \text{ and } \nabla \delta\mu_{\pm} \text{ are continuous,} \quad (7)$$

where $\boldsymbol{\tau}$ is the viscous stress and \mathbf{e}_r is the unit vector in the r direction. Equation (7) are the continuity requirements of the fluid velocity and stress, electrical potential and field, as well as ionic concentrations and fluxes at the interface. Various boundary conditions describing fluid flow at interfaces between porous media and surrounding fluids are discussed in detail in the literature [35,36] related to Darcy's law and Brinkman's equation, and Equation (7) is physically true and mathematically consistent with Equation (2).

The boundary conditions of the small perturbations at the cavity wall are [26,27]

$$r = b : \quad \mathbf{u} = -U\mathbf{e}_z, \quad \mathbf{e}_r \cdot \nabla \delta\psi = 0, \quad \mathbf{e}_r \cdot \nabla \delta\mu_{\pm} = 0. \quad (8)$$

Equations (6) and (8) take a reference frame moving with the particle and show that the Gauss condition holds at the surfaces of the hard sphere core and cavity wall as well as no ions can penetrate into these surfaces.

Chapter 3

Solution of Electrokinetic Equations



3.1. Equilibrium Electric Potential

For the electrolyte solution around a soft spherical particle whose porous surface layer has a uniform space charge density \bar{Q} located at the center of a spherical cavity with a constant surface charge density σ , the equilibrium electric potential profile satisfying proper boundary conditions was obtained as [37]

$$\psi^{(\text{eq})} = \psi_{\text{eq}01}(r)\bar{Q} + \psi_{\text{eq}10}(r)\bar{\sigma}, \quad (9)$$

where

$$\begin{aligned} \psi_{\text{eq}01}(r) &= \frac{kTe^{-\kappa r}}{2ZeA\kappa r} \{ [e^{\kappa a}(\kappa a - 1)(\kappa r_0 + 1) - e^{\kappa(2r_0-a)}(\kappa a + 1)(\kappa r_0 - 1)][e^{2\kappa b}(\kappa b - 1) \\ &\quad + e^{2\kappa r}(\kappa b + 1)] \} \quad \text{for } a < r < b, \end{aligned} \quad (10a)$$

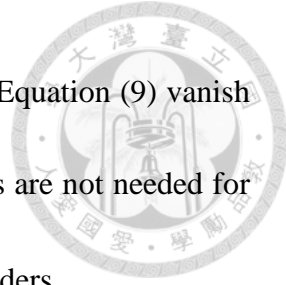
$$\begin{aligned} \psi_{\text{eq}01}(r) &= \frac{kTe^{\kappa(2b-a+2r_0-r)}}{2ZeA\kappa r} \{ \frac{1}{A} + e^{\kappa(a-2b)}(\kappa b + 1)(\kappa r_0 - 1)[e^{\kappa a}(\kappa a - 1) - 2e^{\kappa r}\kappa r] \\ &\quad - e^{\kappa(r-2r_0)}(\kappa b - 1)(\kappa r_0 + 1)[e^{\kappa r}(\kappa a + 1) - 2e^{\kappa a}\kappa r] + e^{2\kappa(a-b-r_0+r)}(\kappa a - 1)(\kappa b + 1) \\ &\quad \times (\kappa r_0 + 1) + \kappa[b - r_0(\kappa b - 1) - a(\kappa b - 1)(\kappa r_0 - 1)] \} \quad \text{for } r_0 < r < a, \end{aligned} \quad (10b)$$

$$\psi_{\text{eq}10}(r) = \frac{2kT(\kappa b)^2 e^{\kappa(b+r_0)}}{ZeA\kappa r} \{ \kappa r_0 \cosh[\kappa(r - r_0)] + \sinh[\kappa(r - r_0)] \}, \quad (11)$$

$$A = e^{2\kappa b}(\kappa b - 1)(\kappa r_0 + 1) - e^{2\kappa r_0}(\kappa b + 1)(\kappa r_0 - 1), \quad (12)$$

$\bar{Q} = ZeQ/\varepsilon\kappa^2 kT$ and $\bar{\sigma} = Ze\sigma/\varepsilon\kappa kT$ are the dimensionless fixed charge densities, and

$\kappa^{-1} = (\varepsilon kT / 2Z^2 e^2 n_0^\infty)^{1/2}$ is the Debye screening length. Note that the contributions of the



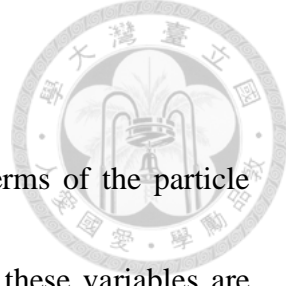
second-order fixed charge densities (\bar{Q}^2 , $\bar{Q}\bar{\sigma}$, and $\bar{\sigma}^2$) to $\psi^{(eq)}$ in Equation (9) vanish for the case of symmetric electrolytes and higher order contributions are not needed for the calculation of the particle sedimentation velocity to the second orders.

Experimental data on porous surface layers of poly(*N*-isopropylacrylamide) hydrogels [38], rat lymphocytes [31], and human erythrocytes [32] in electrolyte solutions show that Q has the magnitude of 10^7 C/m^3 . For σ , experimental studies on AgI surfaces in aqueous solution show that it ranges from 0 to 0.035 C/m^2 when pAg increases from 5.6 to 11 [39]. For the system of soft particles inside a cavity filled with the aqueous solution of monovalent electrolytes with $\kappa^{-1} = 1 \text{ nm}$, $Q = 10^7 \text{ C/m}^3$, and $\sigma = 0.01 \text{ C/m}^2$, the dimensionless fixed charge densities $\bar{Q} \cong \bar{\sigma} \cong 0.5$ are obtained.

Substituting Equations (9)-(12) into the Gauss condition at $r = b$, we obtain the following relation between the zeta potential ζ and the surface charge density σ of the cavity wall confining the soft sphere:

$$\begin{aligned} & \{\kappa r_0 \cosh[\kappa(b - r_0)] + \sinh[\kappa(b - r_0)]\} \kappa^2 b \sigma \\ &= \{\kappa(b - r_0) \cosh[\kappa(b - r_0)] + (\kappa^2 b r_0 - 1) \sinh[\kappa(b - r_0)]\} \varepsilon \kappa^2 \zeta \\ & - \{\kappa(a - r_0) \cosh[\kappa(a - r_0)] + (\kappa^2 a r_0 - 1) \sinh[\kappa(a - r_0)]\} Q. \end{aligned} \quad (13)$$

Namely, $\psi^{(eq)}$ expressed by Equation (9) after substituting Equation (13) is still valid for the case of constant zeta potential at the cavity wall.



3.2. Small Perturbations

To solve the small perturbations \mathbf{u} , δp , $\delta\psi$, and $\delta\mu_{\pm}$ in terms of the particle velocity U for small dimensionless charge densities \bar{Q} and $\bar{\sigma}$, these variables are

expressed as perturbed expansions in powers of \bar{Q} and $\bar{\sigma}$ up to the second orders,

such as

$$U = U_{00} + U_{01}\bar{Q} + U_{10}\bar{\sigma} + U_{02}\bar{Q}^2 + U_{11}\bar{Q}\bar{\sigma} + U_{20}\bar{\sigma}^2, \quad (14)$$

where the coefficients U_{ij} with i and j equal to 0, 1, or 2 to be determined are

independent of \bar{Q} and $\bar{\sigma}$, but are functions of the ratios of core-to-particle radii r_0/a ,

particle-to-cavity radii a/b , particle radius to the Debye length κa , and particle radius to

porous layer permeation length λa . In the expansions of $\delta\psi$ and $\delta\mu_{\pm}$, there is no zeroth-

order term of \bar{Q} and $\bar{\sigma}$ because no ionic concentration gradient or electric field is

applied.

Substituting the expansions of \mathbf{u} , δp , $\delta\psi$, $\delta\mu_{\pm}$, and U in the form of Equation

(14) and Equation (9) for $\psi^{(eq)}$ into Equations (2)-(8), we obtain the following solution

for the components of \mathbf{u} in spherical coordinates, δp (to the orders \bar{Q}^2 , $\bar{Q}\bar{\sigma}$, and

$\bar{\sigma}^2$), $\delta\psi$, and $\delta\mu_{\pm}$ (to the orders \bar{Q} and $\bar{\sigma}$):

$$\begin{aligned} u_r &= \{F_{00r}(r)[U_{00} + U_{01}\bar{Q} + U_{10}\bar{\sigma}] + [U_{02}F_{00r}(r) + U_{00}F_{02r}(r)]\bar{Q}^2 \\ &\quad + [U_{11}F_{00r}(r) + U_{00}F_{11r}(r)]\bar{Q}\bar{\sigma} + [U_{20}F_{00r}(r) + U_{00}F_{20r}(r)]\bar{\sigma}^2\} \cos\theta, \end{aligned} \quad (15a)$$

$$u_{\theta} = -\frac{\tan\theta}{2r} \frac{d}{dr}(r^2 u_r), \quad (15b)$$

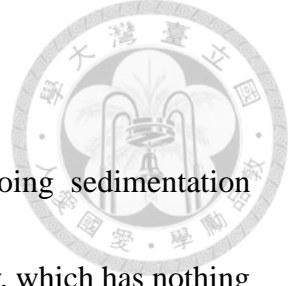


$$\begin{aligned}
\delta p = & \frac{\eta}{a} \{ U_{00} F_{p00}(r) + U_{01} F_{p00}(r) \bar{Q} + U_{10} F_{p00}(r) \bar{\sigma} \\
& + [U_{02} F_{p00}(r) + U_{00} F_{p02}(r) + \frac{a\epsilon\kappa^2}{\eta} U_{00} \psi_{eq01}(r) F_{\psi01}(r)] \bar{Q}^2 \\
& + [U_{11} F_{p00}(r) + U_{00} F_{p11}(r) + \frac{a\epsilon\kappa^2}{\eta} U_{00} \{\psi_{eq01}(r) F_{\psi10}(r) + \psi_{eq10}(r) F_{\psi01}(r)\}] \bar{Q} \bar{\sigma} \\
& + [U_{20} F_{p00}(r) + U_{00} F_{p20}(r) + \frac{a\epsilon\kappa^2}{\eta} U_{00} \psi_{eq10}(r) F_{\psi10}(r)] \bar{\sigma}^2 \} \cos \theta, \quad (15c)
\end{aligned}$$

$$\delta\psi = U_{00} [F_{\psi01}(r) \bar{Q} + F_{\psi10}(r) \bar{\sigma}] \cos \theta, \quad (16)$$

$$\delta\mu_{\pm} = Ze U_{00} [F_{01\pm}(r) \bar{Q} + F_{10\pm}(r) \bar{\sigma}] \cos \theta. \quad (17)$$

Here, the functions $\psi_{eq01}(r)$ and $\psi_{eq10}(r)$ have been given by Equations (10) and (11), and the functions $F_{ijr}(r)$, $F_{pij}(r)$, $F_{\psi ij}(r)$, and $F_{ij\pm}(r)$ are given by Equations (A1)-(A4), (A9), and (A10) in the Appendix A. Because $F_{\psi01}(r)$, $F_{\psi10}(r)$, $F_{01\pm}(r)$, and $F_{10\pm}(r)$ are influenced by the zeroth-order fluid flow field, the leading orders of the relaxation effect on the electrical double layers adjacent to the particle and cavity wall are contained in the solutions for $\delta\psi$ and $\delta\mu_{\pm}$ to the first orders \bar{Q} and $\bar{\sigma}$ (that are sufficient for calculations of the settling velocity to the second orders \bar{Q}^2 , $\bar{Q}\bar{\sigma}$, and $\bar{\sigma}^2$).



3.3. Forces on the Particle

The net force exerted on the soft spherical particle undergoing sedimentation includes the gravity, electrical, and hydrodynamic forces. The gravity, which has nothing to do with the fixed and mobile electric charges, is ,

$$\mathbf{F}_g = \frac{4}{3}\pi[r_0^3(\rho_c - \rho) + (a^3 - r_0^3)(1 - \varepsilon_p)(\rho_p - \rho)]ge_z, \quad (18)$$

where ρ_p and ε_p are the mass density and porosity, respectively, of the surface layer of the particle, ρ and ρ_c are the mass densities of the fluid and hard core, respectively, and ge_z is the gravitational acceleration.

The electrical force acting on the charged soft particle is [26,37]

$$\mathbf{F}_e = 2\pi a^2 \varepsilon \int_0^\pi [\nabla \delta\psi \nabla \psi^{(eq)}]_{r=a} \cdot \mathbf{e}_r \sin \theta d\theta. \quad (19)$$

Substitution of Equations (9) and (16) into Equation (19) results in

$$\begin{aligned} \mathbf{F}_e = & \frac{4}{3}\pi\varepsilon a U_{00} \{ [2F_{\psi 01}(a) \frac{d\psi_{eq01}}{dr}(a) + a \frac{dF_{\psi 01}}{dr}(a) \frac{d\psi_{eq01}}{dr}(a)] \bar{Q}^2 + [2F_{\psi 10}(a) \frac{d\psi_{eq10}}{dr}(a) \\ & + a \frac{dF_{\psi 01}}{dr}(a) \frac{d\psi_{eq10}}{dr}(a) + 2F_{\psi 10}(a) \frac{d\psi_{eq01}}{dr}(a) + a \frac{dF_{\psi 10}}{dr}(a) \frac{d\psi_{eq01}}{dr}(a)] \bar{Q}\bar{\sigma} \\ & + [2F_{\psi 10}(a) \frac{d\psi_{eq10}}{dr}(a) + a \frac{dF_{\psi 10}}{dr}(a) \frac{d\psi_{eq10}}{dr}(a)] \bar{\sigma}^2 \} \mathbf{e}_z. \end{aligned} \quad (20)$$

Only the second orders \bar{Q}^2 , $\bar{Q}\bar{\sigma}$, and $\bar{\sigma}^2$ contribute to \mathbf{F}_e , since both $\delta\psi$ (sedimentation-induced electric potential) and $\psi^{(eq)}$ are of the first orders \bar{Q} and $\bar{\sigma}$.

The hydrodynamic drag force exerted on the soft particle is given by



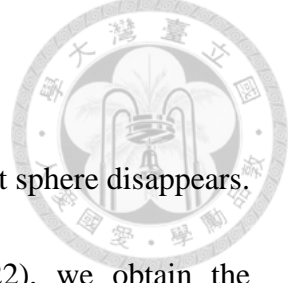
(21)

$$\mathbf{F}_h = 2\pi a^2 \int_0^\pi \{\eta[\nabla \mathbf{u} + \nabla(\mathbf{u})^T] \cdot \mathbf{e}_r - \delta p \mathbf{e}_r\}_{r=a} \sin \theta d\theta.$$

Substitution of Equation (15) into the previous equation leads to

$$\begin{aligned}
 \mathbf{F}_h = & -4\pi \{ \eta a C_{006} (U_{00} + U_{01} \bar{Q} + U_{10} \bar{\sigma}) \\
 & + [\eta a (C_{026} U_{00} + C_{006} U_{02}) + \frac{1}{3} \varepsilon (\kappa a)^2 U_{00} F_{\psi 01}(a) \psi_{eq01}(a)] \bar{Q}^2 \\
 & + [\eta a (C_{116} U_{00} + C_{006} U_{11}) + \frac{1}{3} \varepsilon (\kappa a)^2 U_{00} \{F_{\psi 10}(a) \psi_{eq01}(a) + F_{\psi 01}(a) \psi_{eq10}(a)\}] \bar{Q} \bar{\sigma} \\
 & + [\eta a (C_{206} U_{00} + C_{006} U_{20}) + \frac{1}{3} \varepsilon (\kappa a)^2 U_{00} F_{\psi 10}(a) \psi_{eq10}(a)] \bar{\sigma}^2 \} \mathbf{e}_z, \quad (22)
 \end{aligned}$$

where the coefficients C_{006} , C_{026} , C_{116} , and C_{206} are given in Equations (A1)-(A4).



3.4. Sedimentation Velocity

At the quasi-steady state, the net force acting on the charged soft sphere disappears.

Using this constraint after adding Equations (18), (20), and (22), we obtain the

sedimentation velocity of the particle inside the charged cavity in the expansion form of

Equation (14) with the coefficients as

$$U_{00} = \frac{g}{3\eta a C_{006}} [r_0^3 (\rho_c - \rho) + (a^3 - r_0^3)(1 - \varepsilon_p)(\rho_p - \rho)], \quad (23)$$

$$U_{01} = 0, \quad (24a)$$

$$U_{10} = 0, \quad (24b)$$

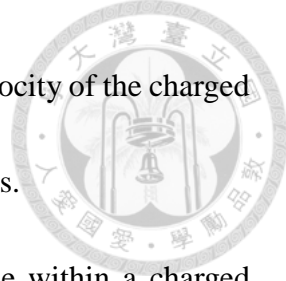
$$\begin{aligned} U_{02} = & -\frac{U_{00}}{C_{006}} [C_{026} + \frac{\varepsilon \kappa^2 a}{3\eta} F_{\psi 01}(a) \psi_{eq01}(a) \\ & - \frac{2\varepsilon}{3\eta} F_{\psi 01}(a) \frac{d\psi_{eq01}}{dr}(a) - \frac{\varepsilon a}{3\eta} \frac{dF_{\psi 01}}{dr}(a) \frac{d\psi_{eq01}}{dr}(a)], \end{aligned} \quad (25a)$$

$$\begin{aligned} U_{11} = & -\frac{U_{00}}{C_{006}} \{C_{116} + \frac{\varepsilon \kappa^2 a}{3\eta} [F_{\psi 10}(a) \psi_{eq01}(a) + F_{\psi 01}(a) \psi_{eq10}(a)] \\ & - \frac{2\varepsilon}{3\eta} [F_{\psi 10}(a) \frac{d\psi_{eq01}}{dr}(a) + F_{\psi 01}(a) \frac{d\psi_{eq10}}{dr}(a)] \\ & - \frac{\varepsilon a}{3\eta} [\frac{dF_{\psi 10}}{dr}(a) \frac{d\psi_{eq01}}{dr}(a) + \frac{dF_{\psi 01}}{dr}(a) \frac{d\psi_{eq10}}{dr}(a)]\}, \end{aligned} \quad (25b)$$

$$\begin{aligned} U_{20} = & -\frac{U_{00}}{C_{006}} [C_{206} + \frac{\varepsilon \kappa^2 a}{3\eta} F_{\psi 10}(a) \psi_{eq10}(a) \\ & - \frac{2\varepsilon}{3\eta} F_{\psi 10}(a) \frac{d\psi_{eq10}}{dr}(a) - \frac{\varepsilon a}{3\eta} \frac{dF_{\psi 10}}{dr}(a) \frac{d\psi_{eq10}}{dr}(a)], \end{aligned} \quad (25c)$$

where U_{00} is the settling velocity of an uncharged soft spherical particle inside a

concentric uncharged spherical cavity [40], which is positive but smaller than that in an



unbounded fluid. As expected, the correction to the sedimentation velocity of the charged soft sphere begins with the second orders of the fixed charge densities.

The sedimentation velocity of a charged soft spherical particle within a charged cavity given by Equations (14) and (23)-(25) can also be expressed as

$$U = U_{00} [1 + H_1(\kappa a)^4 \bar{Q}^2 + H_2(\kappa a)^3 \bar{Q} \bar{\sigma} + H_3(\kappa a)^2 \bar{\sigma}^2], \quad (26)$$

where

$$H_1 = \frac{U_{02}}{U_{00}(\kappa a)^4}, \quad (27a)$$

$$H_2 = \frac{U_{11}}{U_{00}(\kappa a)^3}, \quad (27b)$$

$$H_3 = \frac{U_{20}}{U_{00}(\kappa a)^2}. \quad (27c)$$

Note that $(\kappa a)\bar{\sigma}$ and $(\kappa a)^2 \bar{Q}$ do not depend on κ or n^∞ . For a soft sphere undergoing sedimentation inside a cavity filled with a symmetric electrolyte solution, the dimensionless second-order coefficients H_1 , H_2 , and H_3 are functions of the ratios of core-to-particle radii r_0/a , particle-to-cavity radii a/b , particle radius to Debye length κa , and particle radius to porous layer permeation length λa .

The terms involving the coefficients H_1 and H_3 can be viewed as the corrections to the sedimentation of a charged soft spherical particle inside a concentric uncharged spherical cavity ($\sigma=0$) and an uncharged soft particle ($Q=0$) inside a concentric charged cavity, respectively. The surface charges of the cavity wall alter the settling



velocity of the soft sphere by means of an electroosmotic recirculating flow developed from interactions of the electrical potential gradient caused by the sedimentation with the electrical double layer adjoining the cavity wall and a wall-induced electrical potential on the soft sphere. In the limiting case of $r_0/a = 0$, Equation (26) reduces to the sedimentation velocity formula for a charged porous spherical particle within a concentric charged cavity.

Chapter 4

Results and Discussion



The sedimentation velocity of a charged soft spherical particle within a concentric charged spherical cavity full of the solution of a symmetric electrolyte is expressed by Equations (26) and (27) as a power expansion of the fixed charge densities of its porous surface layer Q and the cavity wall σ up to the second orders Q^2 , $Q\sigma$, and σ^2 .

4.1. The Coefficient H_1 , H_2 , and H_3

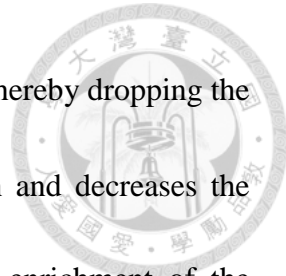
For the settling of a soft particle within a cavity filled with an aqueous solution of potassium chloride (KCl, with $\varepsilon k^2 T^2 / \eta D_{\pm} Z^2 e^2 = 0.26$ at room temperature), the coefficients H_1 , H_2 , and H_3 calculated from Equations (25) and (27), are plotted versus the ratios of particle-to-cavity radii a/b , particle radius to the Debye length κa , particle radius to porous layer permeation length λa , and core-to-particle radii r_0/a in Figures 2-4 for a wide range

The coefficient H_1 (and U_{02}) is negative, so the presence of stationary space charges in the porous surface layer of the soft sphere reduces its sedimentation velocity. This retarding effect is caused by the electrophoresis in the opposite direction generated by the sedimentation-induced electrical potential field, as given by Equation (16). For



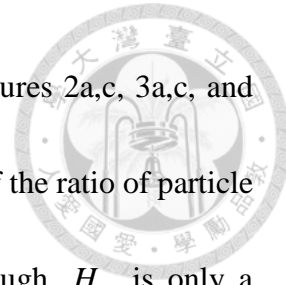
specified values of λa , κa , and r_0/a , as shown in Figures 2b and 2d, $-H_1$ first increases with an increase in the particle-to-cavity radius ratio a/b , reaches a maximum, and then decreases with a further increase in a/b . It is understood that both $-U_{02}$ and U_{00} given by Equations (25a) and (23) are monotonic decreasing functions of a/b , due to the electrophoretic and viscous retardation effects, respectively, of the cavity wall on the moving soft sphere. Compared to U_{00} , $-U_{02}$ decreases slow for low value of a/b and fast for high value of a/b , causing $-H_1$ to reach a maximum according to Equation (27a). As κa increases or λa decreases, the position of this maximum moves to larger a/b .

Both coefficients H_2 and H_3 are positive, so the contribution of H_3 from σ^2 increases the settling velocity of an uncharged soft sphere in the cavity. The counterion concentration in the electric double layer adjoining the cavity wall near the front side of the settling particle increases because of the squeezing of the fluid, while the counterion concentration near the back side of the soft sphere decreases due to fluid compensation, generating a sedimentation-induced electrical potential gradient and electroosmosis along the cavity wall to enhance the recirculating flow and particle sedimentation. The contribution of H_2 of interactions between the stationary space charge of the porous surface layer of the soft sphere and the surface charge of the cavity wall increases the sedimentation velocity if these charges have the same sign ($Q\sigma > 0$, counterions near the



particle surface and cavity wall are reduced by mutual competition, thereby dropping the sedimentation-induced electric field and electrophoretic retardation and decreases the particle velocity if these charges are opposite in sign ($Q\sigma < 0$, enrichment of the counterions in the double layers enhances the induced potential gradient and electrophoretic retardation. For given values of λa , κa , and r_0/a , as shown in Figures 3b,d and 4b,d, the coefficients H_2 and H_3 are decreasing functions of the particle-to-cavity radius ratio a/b (because the increase of a/b decreases the surface area of the cavity for a given particle and therefore reduces the effect of cavity surface charge on the settling particle).

For fixed values of λa , a/b , and r_0/a , as shown in Figures 2a, 3a, and 4a, the coefficients $-H_1$, H_2 , and H_3 have maxima at some finite values of the ratio of particle radius to Debye length κa and gradually fade as κa becomes smaller or larger. In general, as a/b increases, the location of these maxima shifts to larger κa , but is insensitive to changes in λa . In the limiting case of very thick double layers ($\kappa a \rightarrow 0$), the counterions in them are negligible and the particle sedimentation is not affected by the interaction between the space charge of the porous surface layer of the soft sphere and the surface charge of the cavity wall. In the case of very thin double layers ($\kappa a \rightarrow \infty$), the charge density vanishes everywhere in fluid and the interaction between fixed charges disappears.



For specified values of a/b , r_0/a , and κa , as shown in Figures 2a,c, 3a,c, and 4a,c, the coefficients $-H_1$, H_2 , and H_3 are decreasing functions of the ratio of particle radius to porous layer permeation length λa as expected. Although H_3 is only a relatively weak function of λa (the charged cavity wall effect on the settling of the soft particle principally through the electroosmotic recirculating flow has not much to do with the relative permeability of its porous surface layer), H_1 and H_2 can strongly depend on λa .

For given values of κa , λa , and a/b , as shown in Figures 2c,d and 3c,d, the coefficients $-H_1$ and H_2 decrease monotonically and substantially with an increase in the core-to-particle radius ratio r_0/a (i.e., a decrease in the relative volume, and thus total space charge, of the porous surface layer of the soft sphere), as expected. On the other hand, as shown in Figures 4c and 4d, the coefficient H_3 due to the surface charge of the cavity wall (it has little to do with the space charge of the porous surface layer) can be a relatively weak nonmonotonic function of r_0/a . It is understood that, as r_0/a increases, both U_{00} and U_{20} given by Equations (23) and (25c) decrease due to the effects of viscous retardation and mainly electroosmotic recirculation, respectively, of the cavity wall on the moving soft sphere. Compared to U_{00} , U_{20} decreases slower for low values of r_0/a and faster for high values of r_0/a , causing H_3 to reach a maximum according to Equation (27c).

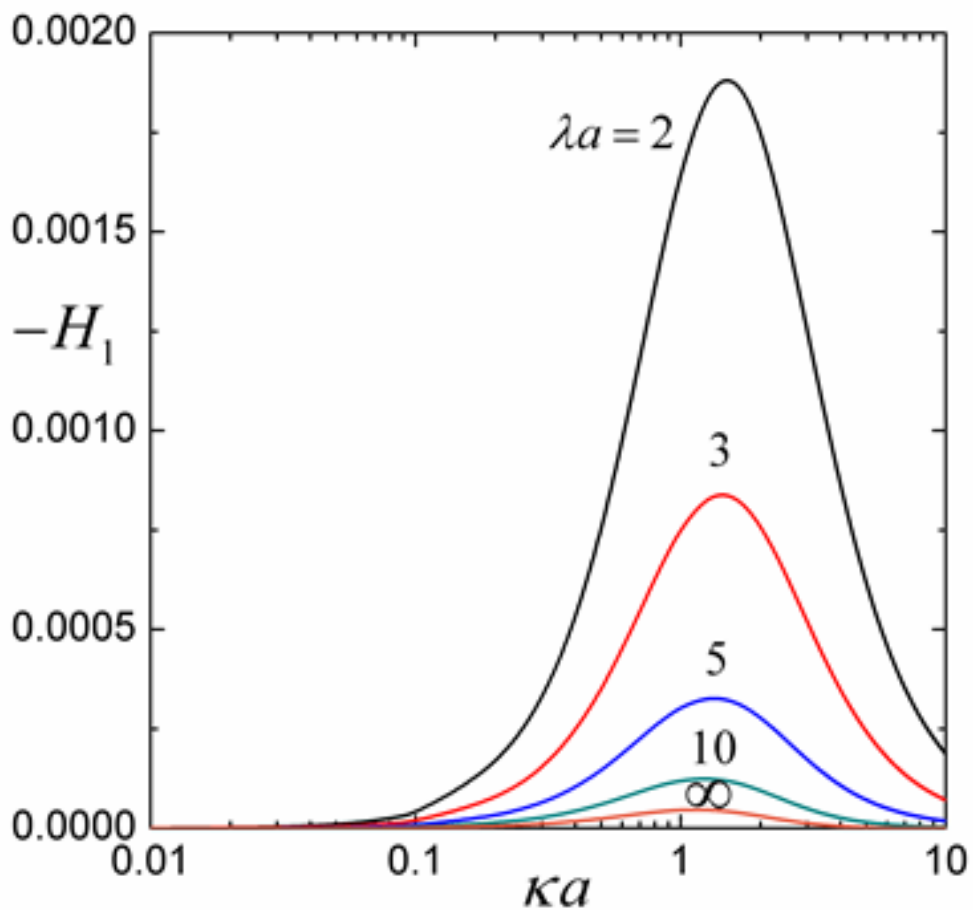


Figure 2a. Plots of the coefficient H_1 in Eq. (26) for the sedimentation of a soft particle in a cavity full of aqueous KCl solution versus the parameter κa with various values of λa at $r_0/a = 0$ and $a/b = 0.5$.

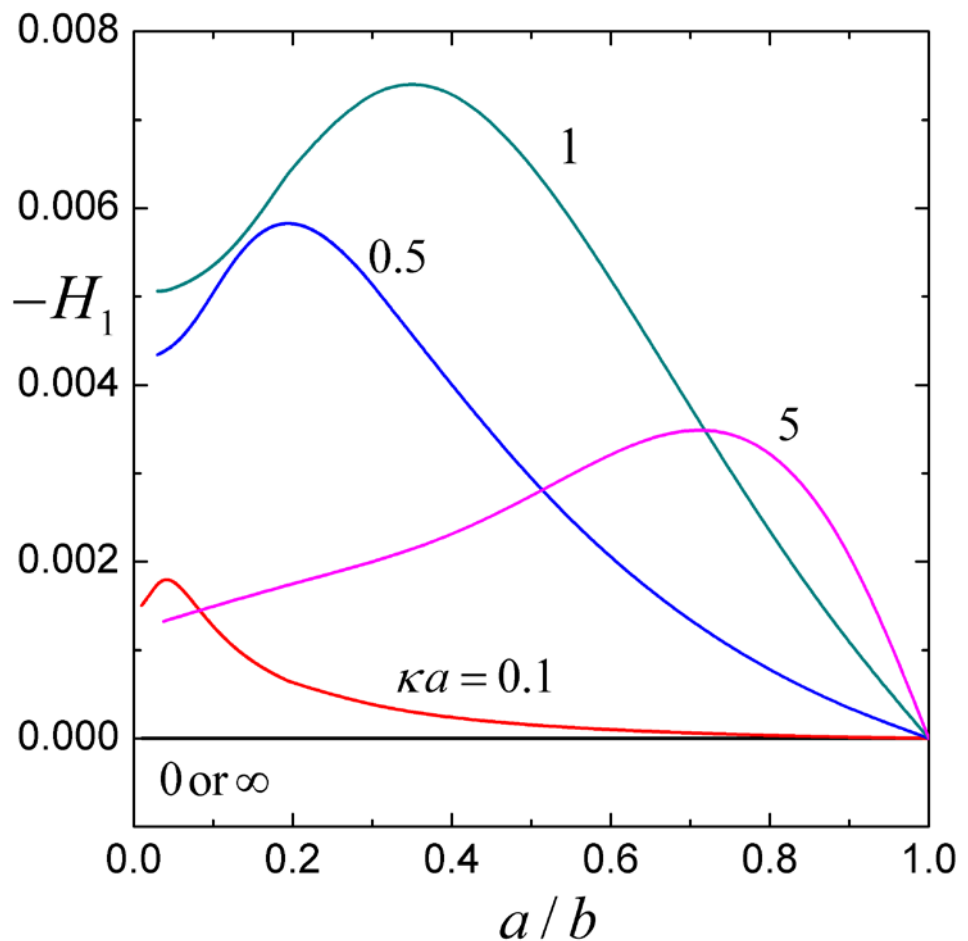


Figure 2b. Plots of the coefficient H_1 in Eq. (26) for the sedimentation of a soft particle in a cavity full of aqueous KCl solution versus the parameter a/b with various values of κa at $r_0/a=0$ and $\lambda a=1$.

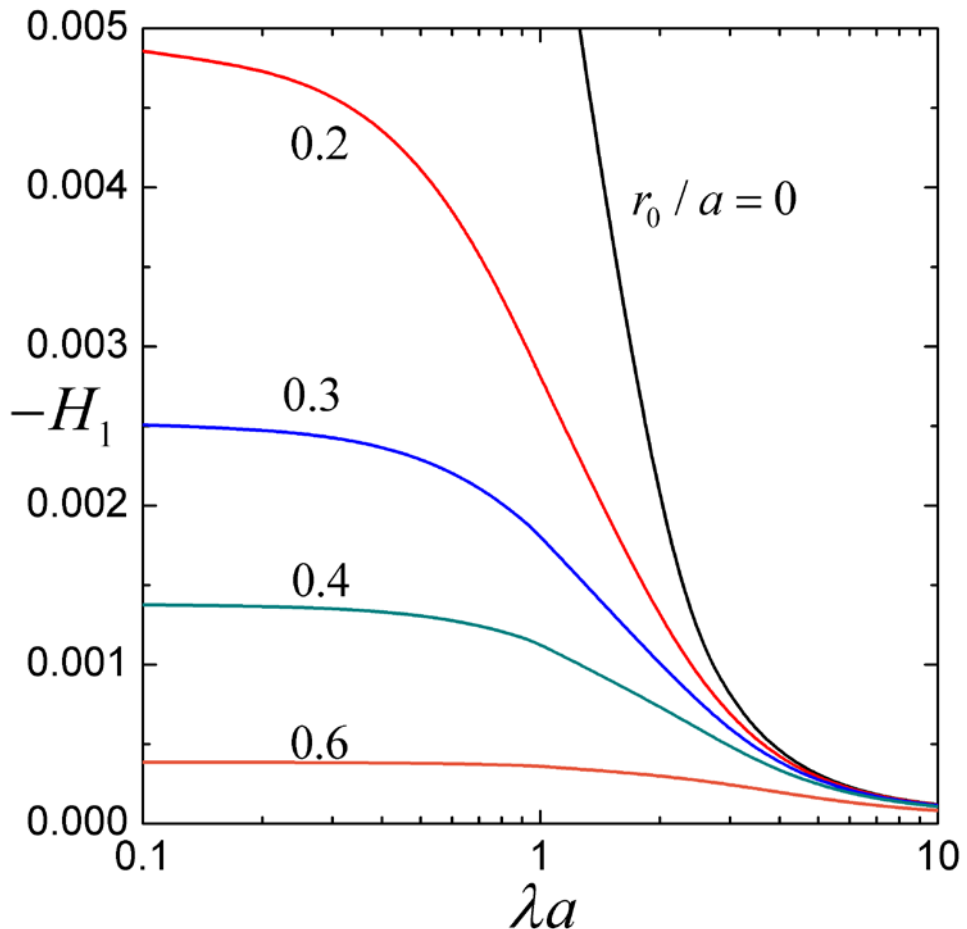


Figure 2c. Plots of the coefficient H_1 in Eq. (26) for the sedimentation of a soft particle

in a cavity full of aqueous KCl solution versus the parameter λa with various values of

r_0 / a at $\kappa a = 1$ and $a / b = 0.5$.

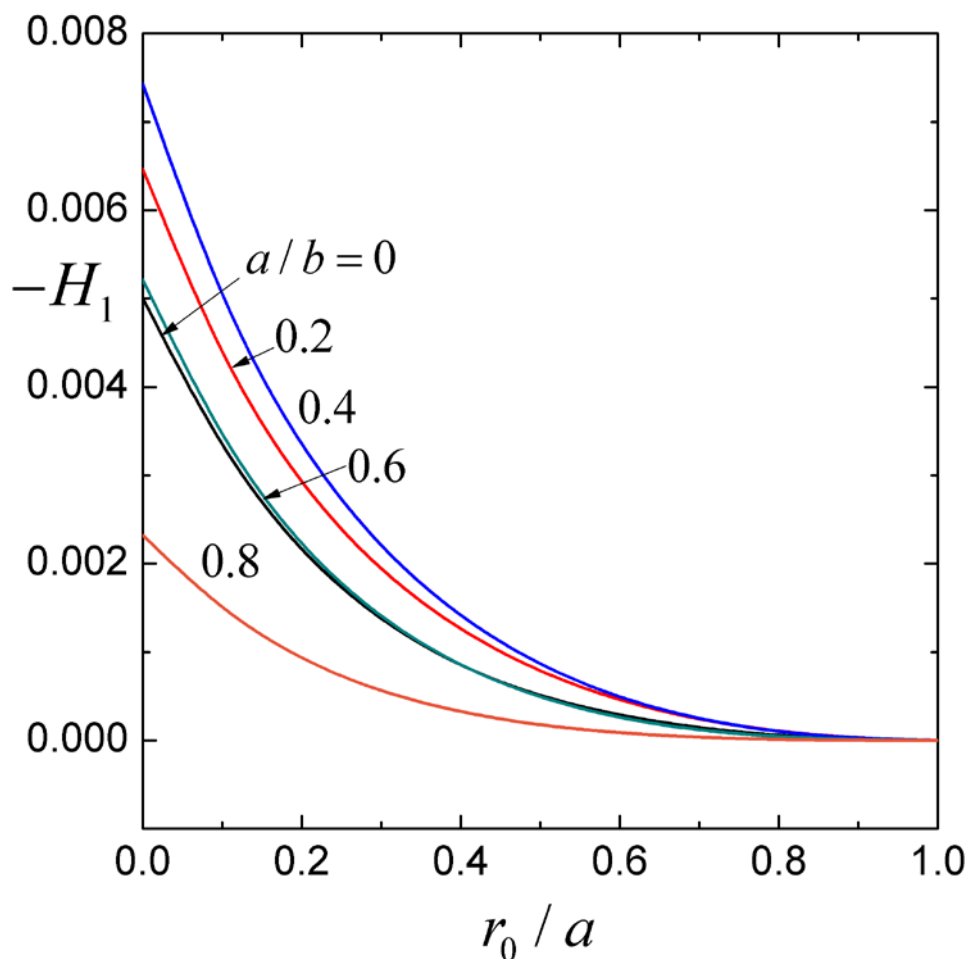


Figure 2d. Plots of the coefficient H_1 in Eq. (26) for the sedimentation of a soft particle in a cavity full of aqueous KCl solution versus the parameter r_0 / a with various values of a / b at $\kappa a = 1$ and $\lambda a = 1$.

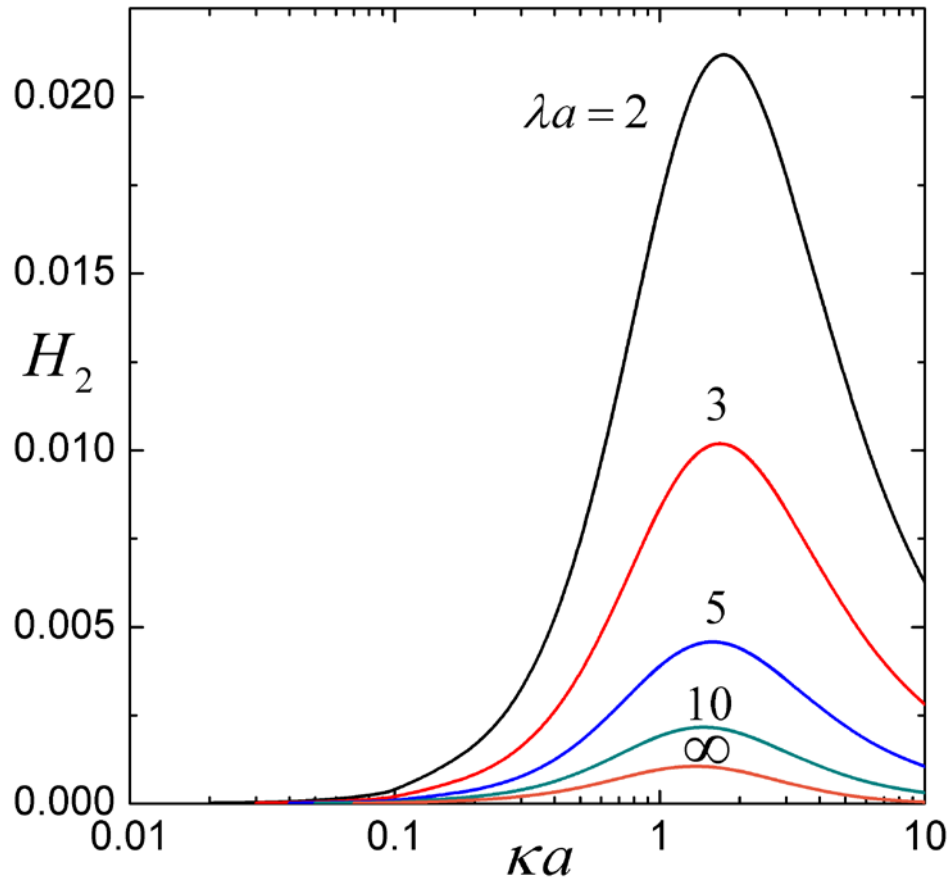


Figure 3a. Plots of the coefficient H_2 in Eq. (26) for the sedimentation of a soft particle in a cavity full of aqueous KCl solution versus the parameter κa with various values of λa at $r_0/a = 0$ and $a/b = 0.5$.

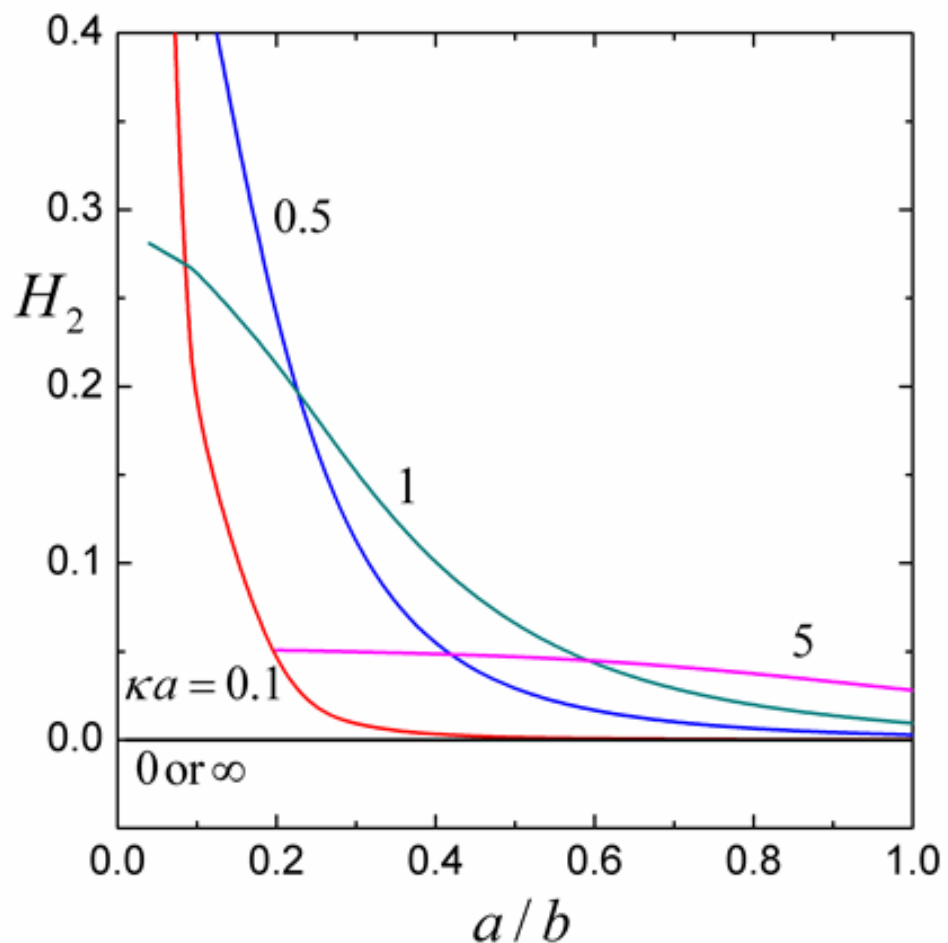
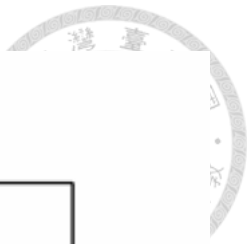


Figure 3b. Plots of the coefficient H_2 in Eq. (26) for the sedimentation of a soft particle in a cavity full of aqueous KCl solution versus the parameter a/b with various values of κa at $r_0/a = 0$ and $\lambda a = 1$.

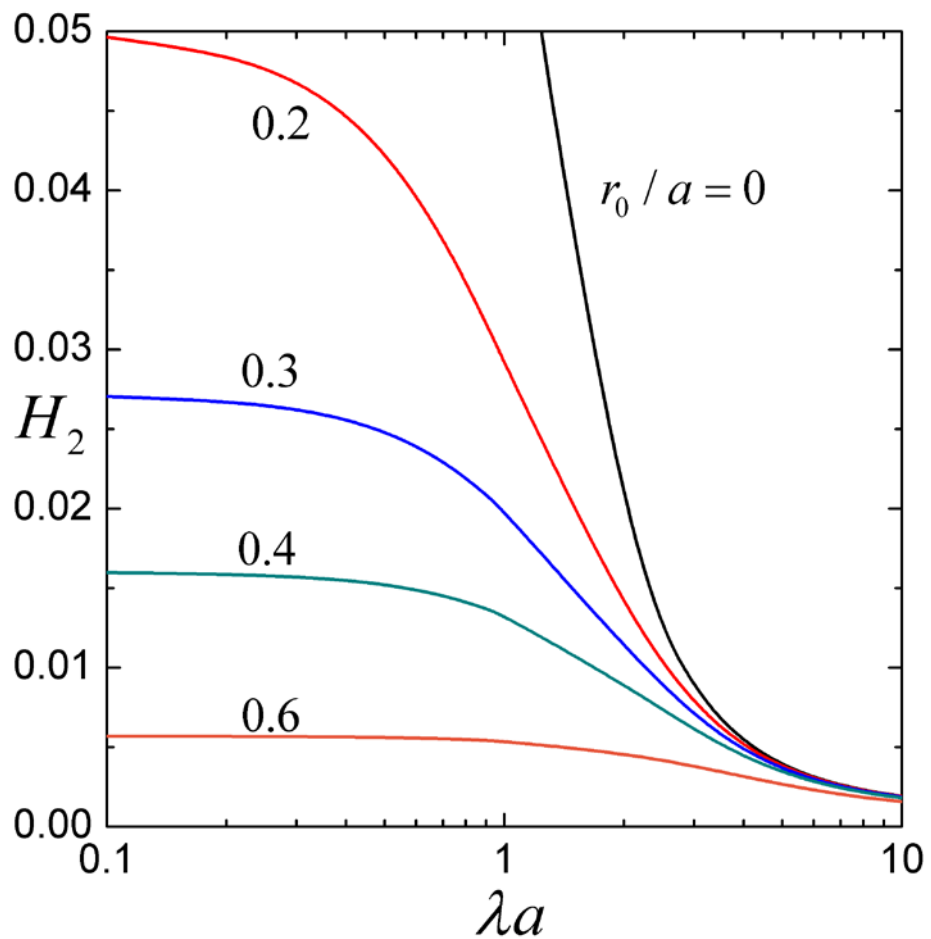


Figure 3c. Plots of the coefficient H_2 in Eq. (26) for the sedimentation of a soft particle

in a cavity full of aqueous KCl solution versus the parameter λa with various values of

r_0 / a at $\kappa a = 1$ and $a / b = 0.5$.

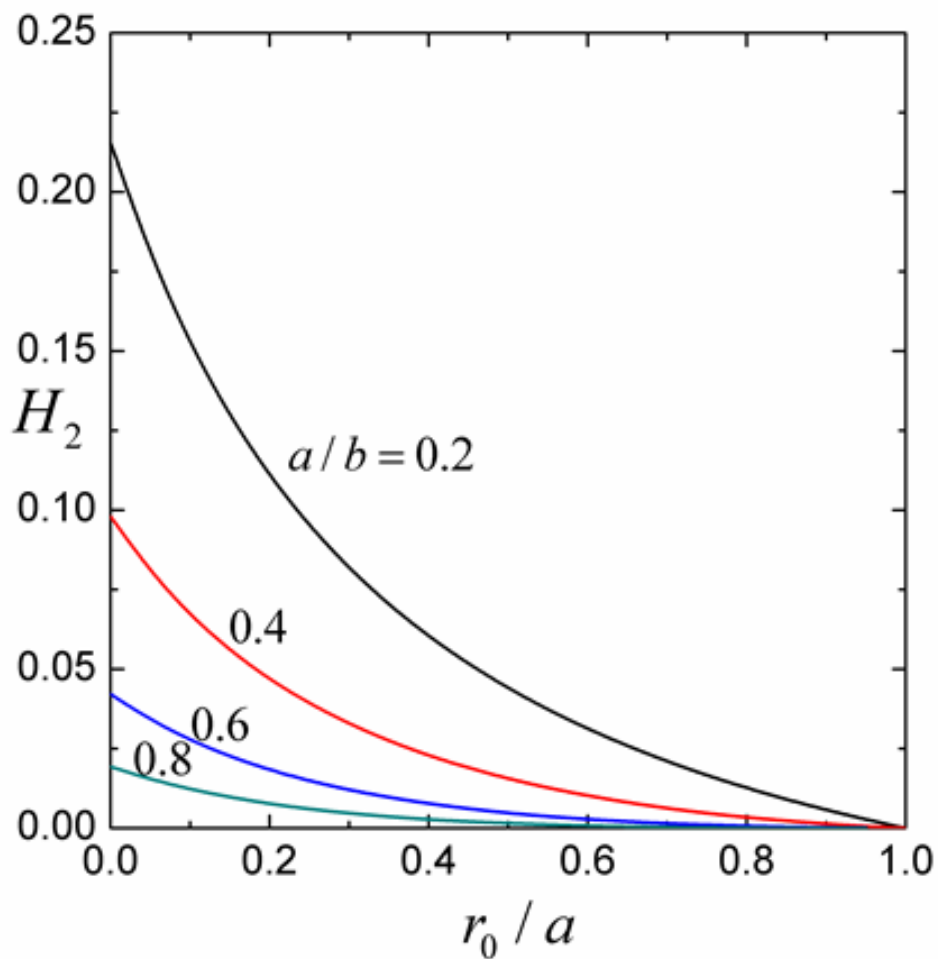


Figure 3d. Plots of the coefficient H_2 in Eq. (26) for the sedimentation of a soft particle in a cavity full of aqueous KCl solution versus the parameter r_0 / a with various values of a/b at $\kappa a = 1$ and $\lambda a = 1$.

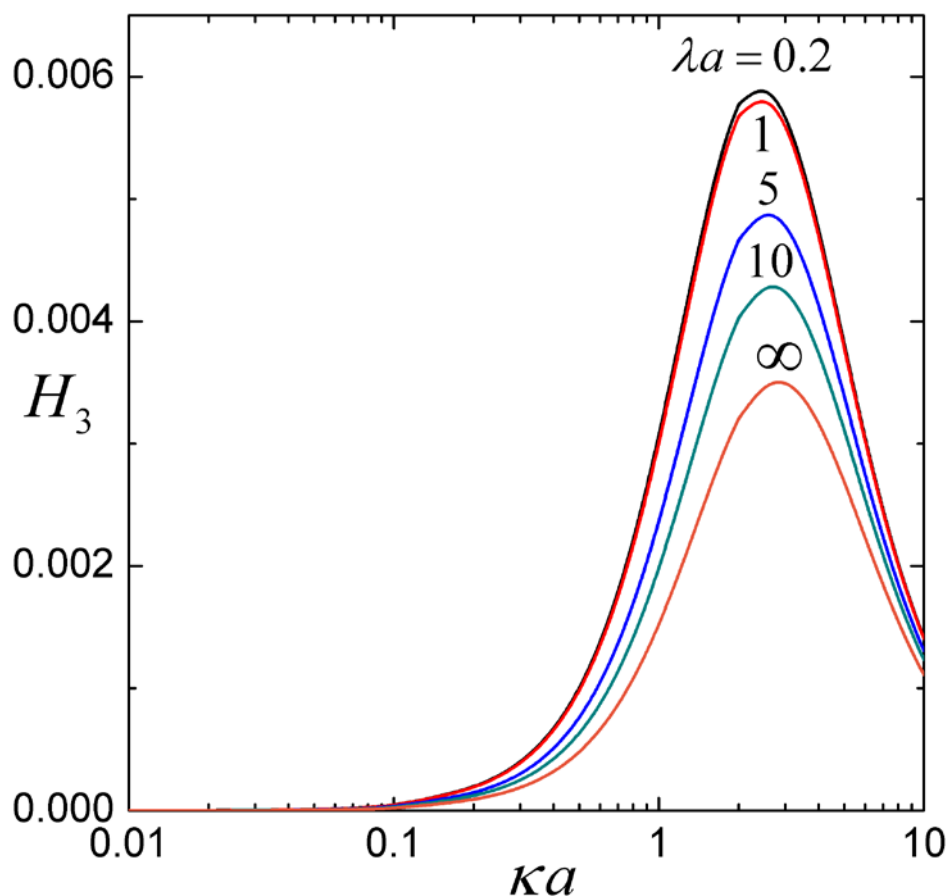


Figure 4a. Plots of the coefficient H_3 in Eq. (26) for the sedimentation of a soft particle in a cavity full of aqueous KCl solution versus the parameter κa with various values of λa at $r_0/a = 0$ and $a/b = 0.5$.

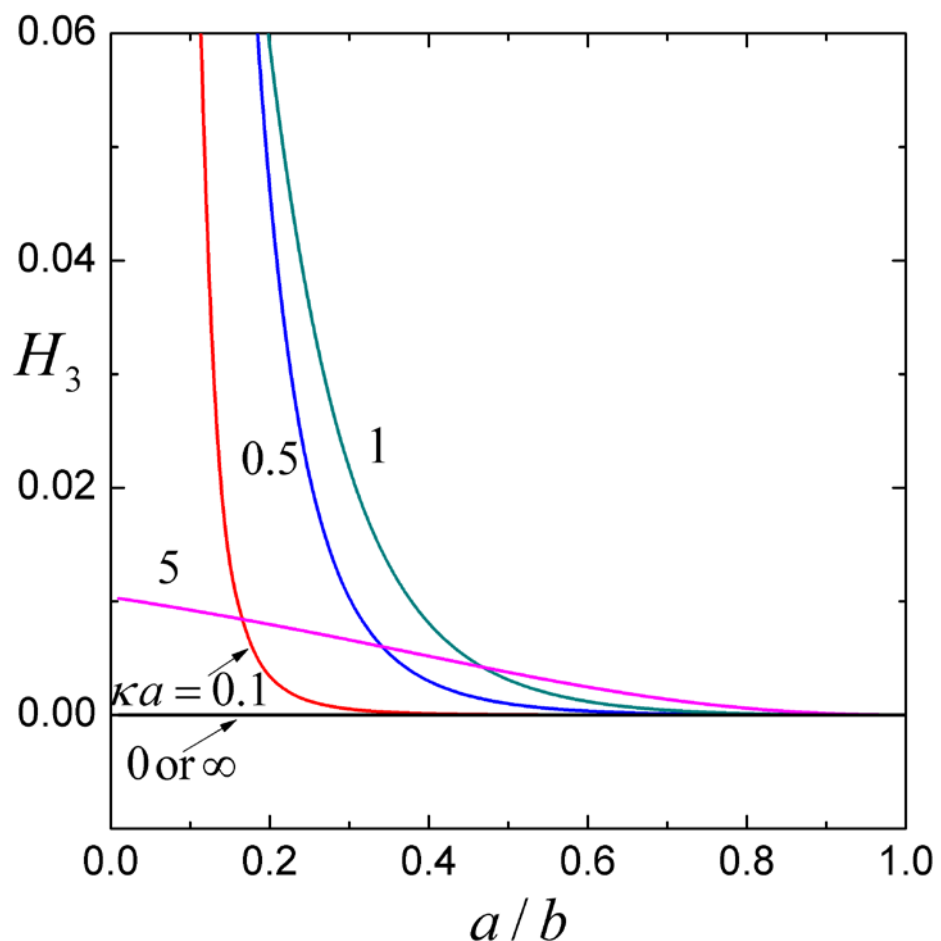


Figure 4b. Plots of the coefficient H_3 in Eq. (26) for the sedimentation of a soft particle in a cavity full of aqueous KCl solution versus the parameter a / b with various values of κa at $r_0 / a = 0$ and $\lambda a = 1$.

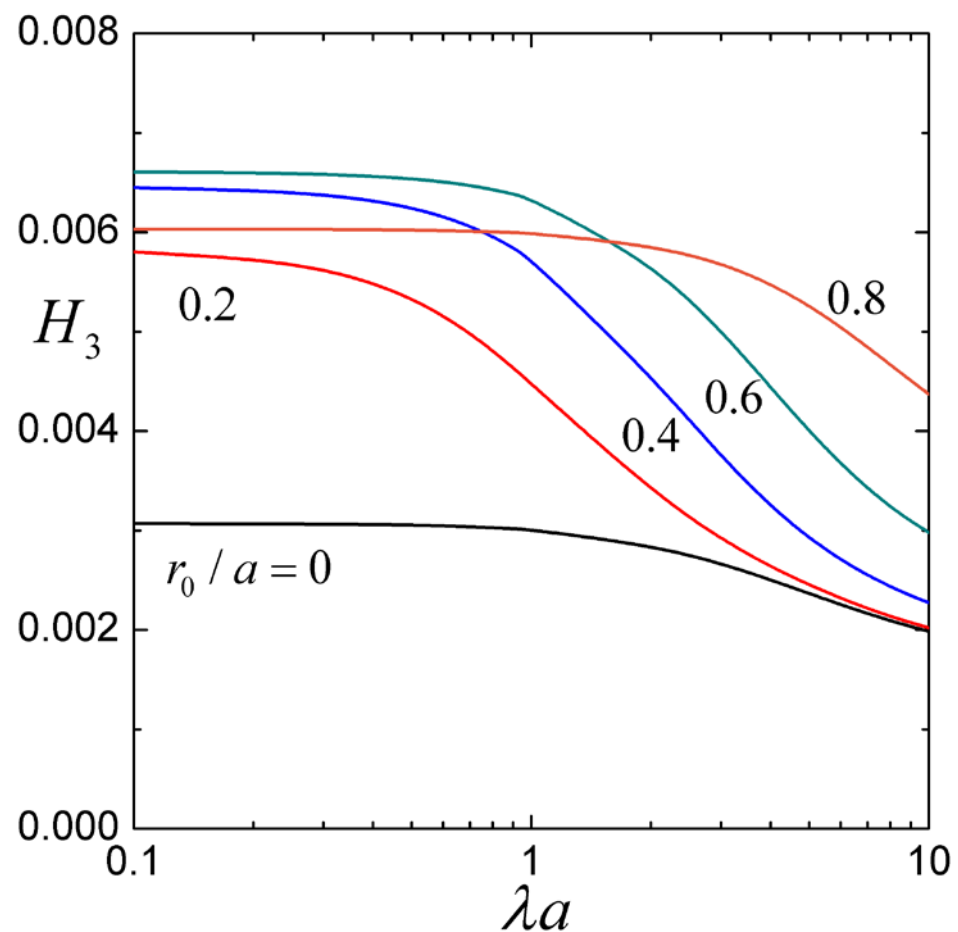


Figure 4c. Plots of the coefficient H_3 in Eq. (26) for the sedimentation of a soft particle in a cavity full of aqueous KCl solution versus the parameter λa with various values of r_0 / a at $\kappa a = 1$ and $a / b = 0.5$.

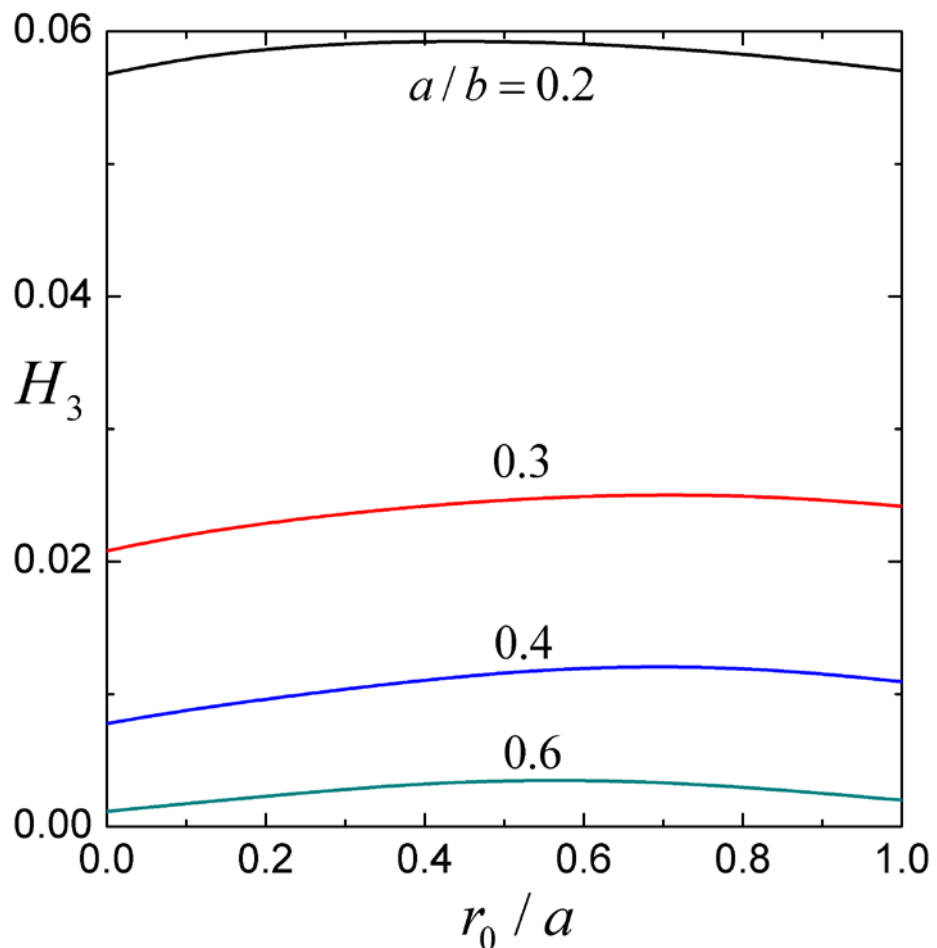


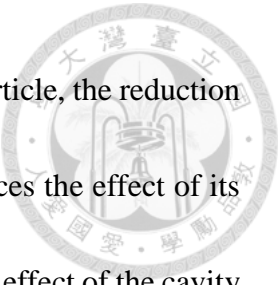
Figure 4d. Plots of the coefficient H_3 in Eq. (26) for the sedimentation of a soft particle in a cavity full of aqueous KCl solution versus the parameter r_0/a with various values of a/b at $\kappa a = 1$ and $\lambda a = 1$.



4.2. The Normalized Sedimentation Velocity

Our results in Figures 2-4 show that the coefficient H_2 in Equation (26) is an order of magnitude larger than the other coefficients $-H_1$ and H_3 . Consequently, for a charged soft spherical particle migrating inside a spherical cavity with a surface charge of the same sign ($Q\sigma > 0$), the net effect of these coefficients is generally to increase the sedimentation velocity of the particle (with exceptions occurring as $|\bar{\sigma}|$ is much smaller than $|\bar{Q}|$ in magnitude). For the case of the cavity with a surface charge of opposite sign ($Q\sigma < 0$), if $|\bar{\sigma}|$ is sufficiently larger/smaller than $|\bar{Q}|$, the net effect is to enhance/reduce the settling velocity. This trend is manifested in Figure 5, which is a plot of the normalized particle velocity U/U_{00} of a soft spherical particle with a space charge density in its porous surface layer $\bar{Q}=1$ inside a spherical cavity full of an aqueous solution of potassium chloride calculated using Equation (26) versus the surface charge density $\bar{\sigma}$ of the cavity wall. The enhancement and reduction of the particle velocity caused by the cavity wall can be substantial if $|\bar{\sigma}|$ is relatively large, especially in cases of small core-to-particle radius ratio r_0/a , ratio of particle radius to porous layer permeation length λa , and particle-to-cavity radius ratio a/b with moderate values of ratio of particle radius to Debye length κa .

Figures 3b,d, 4b,d, and 5a show that the influence of the charged cavity wall on the sedimentation of the soft sphere increases as a/b decreases, with other parameters



remaining constant. This result reflects the fact that for a fixed size particle, the reduction of a/b increases the surface area of the cavity and therefore enhances the effect of its surface charge on the settling particle. Figures 5b,c,d illustrate that the effect of the cavity wall surface charge on the sedimentation of the soft sphere increases with decreases in r_0/a and λa , but is not a monotonic function of κa .

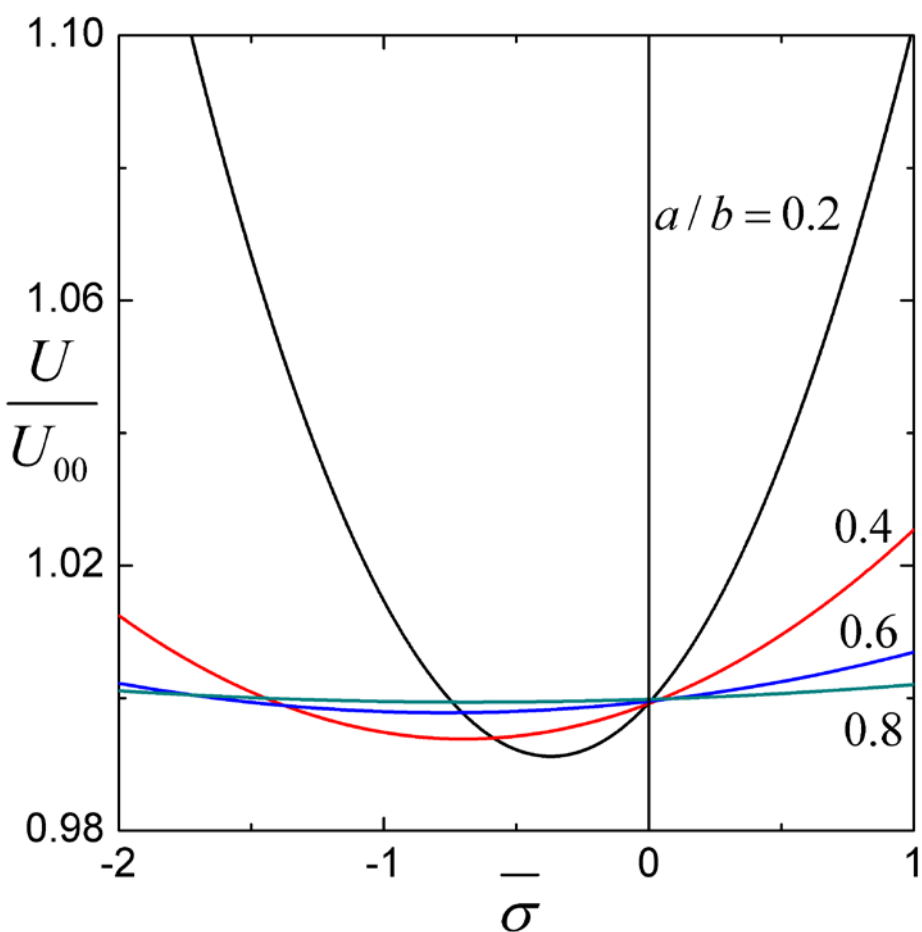


Figure 5a. Plots of the normalized sedimentation velocity U / U_{00} of a soft particle with $\bar{Q} = 1$ in a cavity full of aqueous KCl solution with $r_0 / a = 0.5$, $\lambda a = 1$, and $\kappa a = 1$ versus the parameter $\bar{\sigma}$ for various values of a/b .

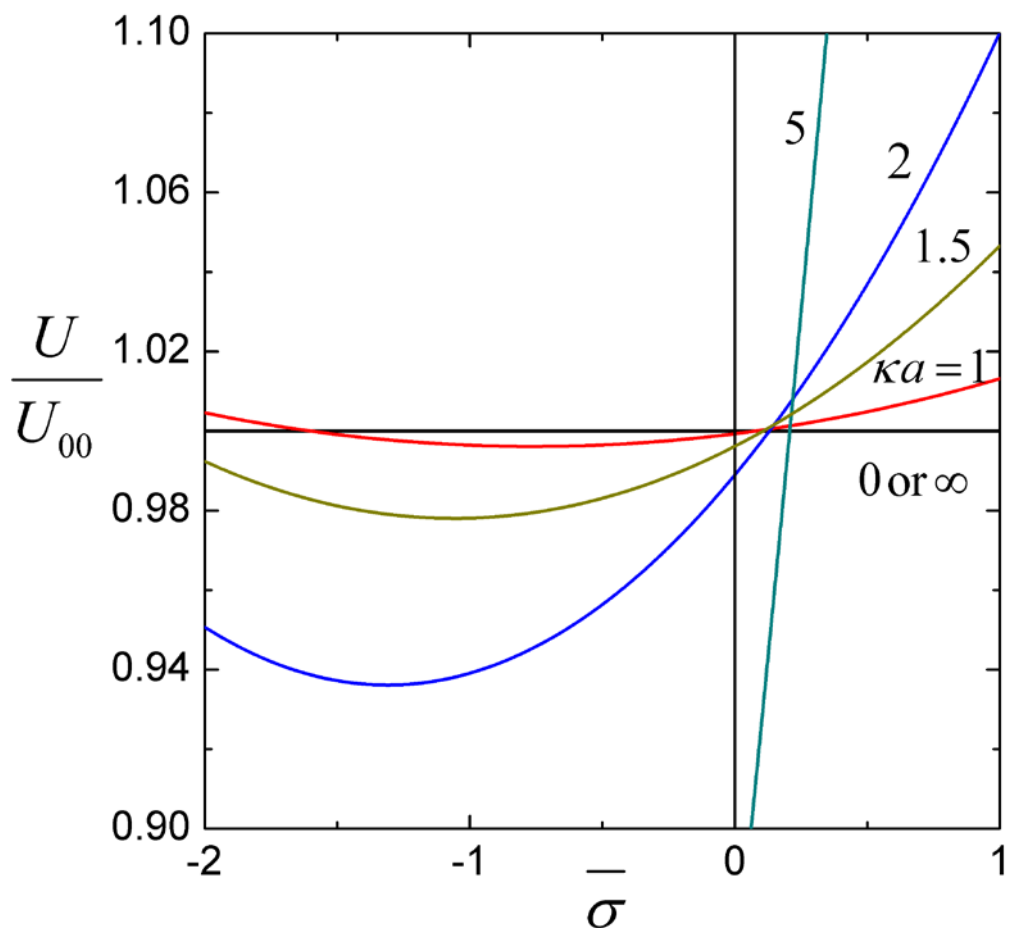


Figure 5b. Plots of the normalized sedimentation velocity U / U_{00} of a soft particle with $\bar{Q} = 1$ in a cavity full of aqueous KCl solution with $r_0 / a = 0.5$, $a / b = 0.5$, and $\lambda a = 1$ versus the parameter $\bar{\sigma}$ for various values of κa .

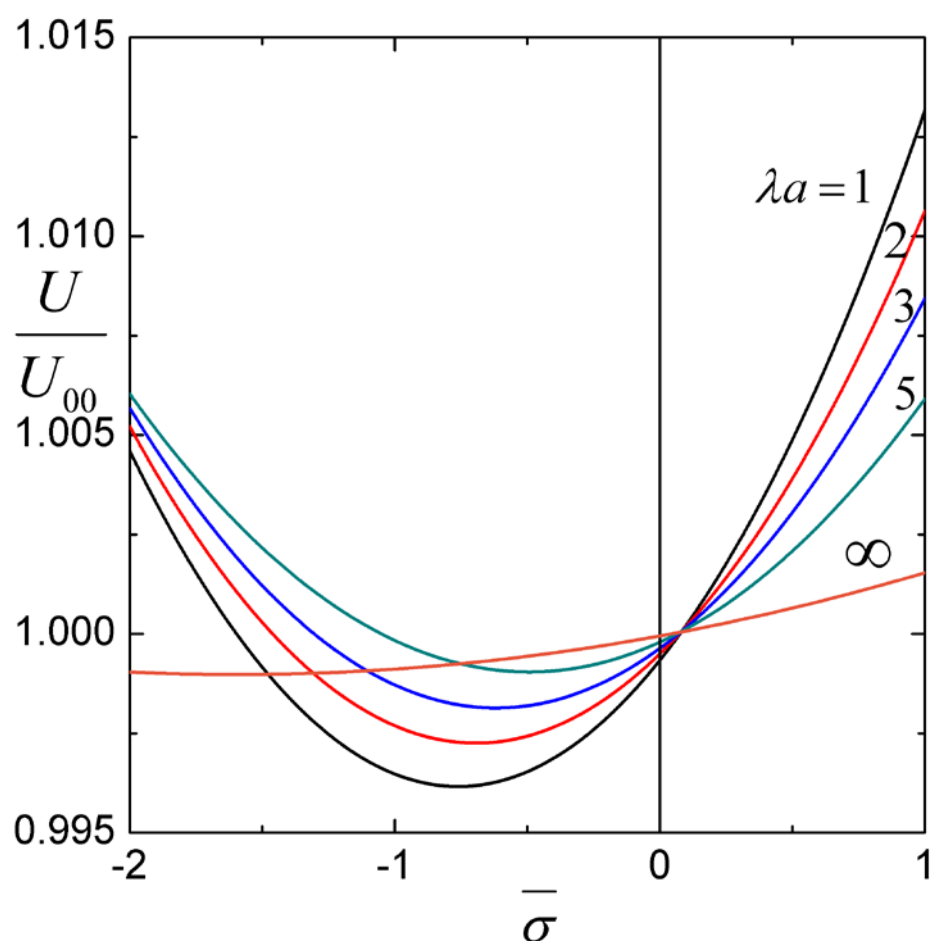


Figure 5c. Plots of the normalized sedimentation velocity U / U_{00} of a soft particle with $\bar{Q} = 1$ in a cavity full of aqueous KCl solution with $r_0 / a = 0.5$, $a / b = 0.5$, and $\kappa a = 1$ versus the parameter $\bar{\sigma}$ for various values of λa .

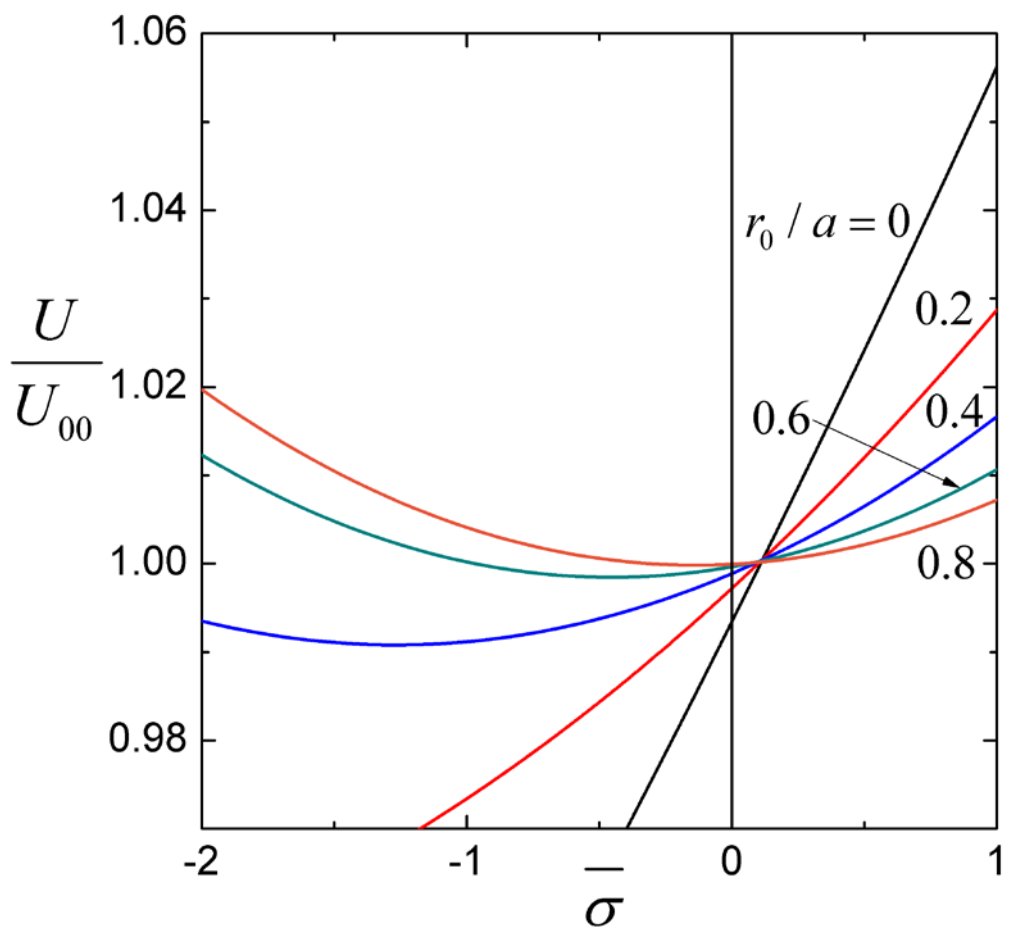


Figure 5d. Plots of the normalized sedimentation velocity U / U_{00} of a soft particle with $\bar{Q} = 1$ in a cavity full of aqueous KCl solution with $a/b = 0.5$, $\lambda a = 1$, and $\kappa a = 1$ versus the parameter $\bar{\sigma}$ for various values of r_0 / a .

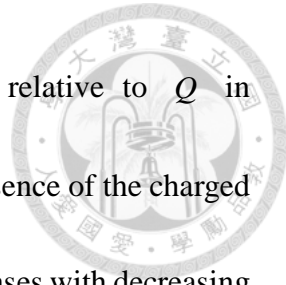
Chapter 5

Conclusions



This thesis presents an analysis of the sedimentation of a soft spherical particle inside a concentric spherical cavity filled with a symmetric electrolyte solution. By using a regular perturbation method with small fixed charge densities of the porous surface layer of the soft sphere Q and cavity wall σ , a set of linearized electrokinetic equations related to the fluid velocity field, electrical potential profile, and ionic electrochemical potential energy distributions are solved with the relaxation effect of the electric double layers. A closed-form formula for the settling velocity of the soft sphere is given by Equation (26) as a function of the ratios of particle-to-cavity radii a/b , particle radius to the Debye length κa , particle radius to porous layer permeation length λa , and core-to-particle radii r_0/a .

Corrections due to the effect of the fixed charges Q and σ on the sedimentation velocity start from the second orders Q^2 , $Q\sigma$, and σ^2 . The existence of the surface charge on the cavity wall increases the settling velocity of the charged soft sphere, mainly because of the electroosmotic enhancement of recirculating flow within the cavity induced by the sedimentation potential gradient. When Q and σ have the same sign, the particle velocity is generally enhanced by the presence of the cavity. When these fixed



charges have opposite signs and σ is sufficiently large/small relative to Q in magnitude, the particle velocity will be enhanced/reduced by the presence of the charged cavity. The effect of σ on the sedimentation of the soft sphere increases with decreasing a/b , λa , and r_0/a , but has a maximum at some finite values of κa and disappears as κa approaches zero and infinity.



Notation

a	the radius of the soft particle, m
b	the radius of the cavity, m
D_+, D_-	the diffusivities of the cation and anion, $\text{m}^2 \cdot \text{s}^{-1}$
e	the elementary electric charge, C
\mathbf{e}_r	the unit vector in the r-direction
\mathbf{e}_z	the unit vector in the z-direction
$F_{00r}(r), F_{p00}(r)$	the functions defined in Eqs. (A1a), (A1b), (A2a) and (A2b)
$F_{02r}(r), F_{11r}(r), F_{20r}(r)$	the functions defined in Eqs. (A3a) and (A3b)
$F_{p02}(r), F_{p11}(r), F_{p20}(r)$	the functions defined in Eqs. (A4a) and (A4b)
$F_{01\pm}(r), F_{10\pm}(r)$	the functions defined in Eqs. (A9a) and (A9b)
$F_{\psi 01}(r), F_{\psi 10}(r)$	the functions defined in Eqs. (A10a) and (A10b)
\mathbf{F}_e	the electric force acting on the charged soft particle, N
\mathbf{F}_g	the gravitational force acting on the charged soft particle, N
\mathbf{F}_h	the hydrodynamic drag force acting on the charged soft particle, N
g	gravitational acceleration, $\text{m} \cdot \text{s}^{-2}$



$h(r)$	unit step function
H_1, H_2, H_3	dimensionless coefficients for the sedimentation velocity
k	Boltzmann's constant, $\text{J} \cdot \text{K}^{-1}$
$n_m^{(\text{eq})}$	the equilibrium concentrations of type-m ions, m^{-3}
n_m^{∞}	the bulk concentrations of type-m ions, m^{-3}
p	the pressure distribution, $\text{N} \cdot \text{m}^{-2}$
$p^{(\text{eq})}$	the equilibrium pressure distribution, $\text{N} \cdot \text{m}^{-2}$
Q	the fixed charge density within the charged soft particle, $\text{C} \cdot \text{m}^{-3}$
\bar{Q}	non-dimensional fixed charge density of the charged soft particle
(r, θ, ϕ)	spherical coordinates
r_0	the radius of the hard core, m
T	the absolute temperature, K
\mathbf{u}	the fluid velocity distribution, $\text{m} \cdot \text{s}^{-1}$
u_r, u_{θ}	r and θ components, respectively, of \mathbf{u} , $\text{m} \cdot \text{s}^{-1}$
U	the sedimentation velocity of the soft particle, $\text{m} \cdot \text{s}^{-1}$
$U_{00}, U_{01}, U_{10}, U_{02}, U_{11}, U_{20}$	the velocities defined in Eqs. (23), (24) and (25), $\text{m} \cdot \text{s}^{-1}$
Z	the valence of the symmetric electrolyte
z_m	the valence of type-m ions



Greek letters

δn_m	the small deviation from the equilibrium concentration of type-m ions, m^{-3}
$\delta\mu_m$	the linear combination of δn_m and $\delta\psi, \text{J}$
$\delta\psi$	the small deviation from the equilibrium electric potential distribution, V
δp	the small deviation from the equilibrium pressure, $\text{N} \cdot \text{m}^{-2}$
ε	the permittivity of the fluid, $\text{C}^2 \cdot \text{J}^{-1} \cdot \text{m}^{-1}$
ε_p	the porosity of the porous surface layer
η	the viscosity of the fluid, $\text{kg} \cdot \text{m}^{-1} \cdot \text{s}^{-1}$
κ	reciprocal of the Debye screening length, m^{-1}
λ	reciprocal of the characteristic length of flow penetration inside the porous layer, m^{-1}
ρ	the mass density of the fluid, $\text{kg} \cdot \text{m}^{-3}$
ρ_p	the mass density of the charged porous layer, $\text{kg} \cdot \text{m}^{-3}$
σ	the fixed charge density on the spherical cavity, $\text{C} \cdot \text{m}^{-2}$
$\bar{\sigma}$	non-dimensional fixed charge density of on the cavity
ψ	the electric potential distribution, V

$\psi^{(eq)}$

the equilibrium electric potential distribution, V

$\psi_{eq01}, \psi_{eq10},$

the functions defined in Eq. (9), V



Superscripts

(eq) equilibrium state

∞ in the bulk solution

Subscripts

+

the cation

-

the anion

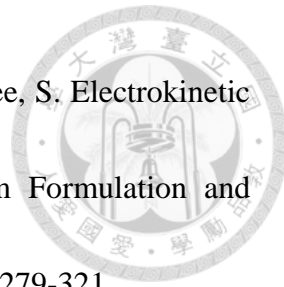
m

the type- m ions

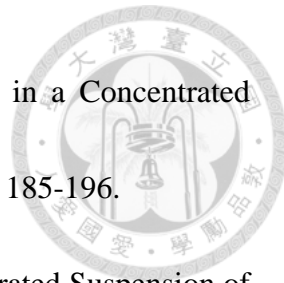
References



1. Adachi, Y. Sedimentation and Electrophoresis of a Porous Floc and a Colloidal Particle Coated with Polyelectrolytes. *Curr. Opin. Colloid Interface Sci.* 2016, 24, 72-78.
2. Satoh, A. Sedimentation Behavior of Dispersions Composed of Large and Small Charged Colloidal Particles: Development of New Technology to Improve the Visibility of Small Lakes and Ponds. *Env. Eng. Sci.* 2015, 32, 528-538.
3. Khair, A. S. Strong Deformation of the Thick Electric Double Layer around a Charged Particle during Sedimentation or Electrophoresis. *Langmuir* 2018, 34, 876-885.
4. Gopmandal, P. P.; Bhattacharyya, S.; Barman, B. Effect of Induced Electric Field on Migration of a Charged Porous Particle. *Eur. Phys. J. E* 2014, 37, 104.
5. Booth, F. Sedimentation Potential and Velocity of Solid Spherical Particles. *J. Chem. Phys.* 1954, 22, 1956-1968.
6. Stigter, D. Sedimentation of Highly Charged Colloidal Spheres. *J. Phys. Chem.* 1980, 84, 2758-2762.
7. Ohshima, H.; Healy, T. W.; White, L. R.; O'Brien, R. W. Sedimentation Velocity and Potential in a Dilute Suspension of Charged Spherical Colloidal Particles. *J. Chem. Soc., Faraday Trans. 2* 1984, 80, 1299-1317.



8. Zholkovskiy, E. K.; Masliyah, J. H.; Shilov, V. N.; Bhattacharjee, S. Electrokinetic Phenomena in Concentrated Disperse Systems: General Problem Formulation and Spherical Cell Approach. *Adv. Colloid Interface Sci.* 2007, 134-135, 279-321.
9. Carrique, F.; Arroyo, F. J.; Delgado, A. V. Sedimentation Velocity and Potential in a Concentrated Colloidal Suspension: Effect of a Dynamic Stern Layer. *Colloids Surfaces A* 2001, 195, 157-169.
10. Keh, H. J.; Ding, J. M. Sedimentation Velocity and Potential in Concentrated Suspensions of Charged Spheres with Arbitrary Double-Layer Thickness. *J. Colloid Interface Sci.* 2000, 227, 540-552.
11. Ohshima, H. Sedimentation Potential in a Concentrated Suspension of Spherical Colloidal Particles. *J. Colloid Interface Sci.* 1998, 208, 295-301.
12. Levine, S.; Neale, G.; Epstein, N. The Prediction of Electrokinetic Phenomena within Multiparticle Systems II. Sedimentation Potential. *J. Colloid Interface Sci.* 1976, 57, 424-437.
13. Keh, H. J.; Chen, W. C. Sedimentation Velocity and Potential in Concentrated Suspensions of Charged Porous Spheres. *J. Colloid Interface Sci.* 2006, 296, 710-720.
14. Hermans, J. J. Sedimentation and Electrophoresis of Porous Spheres. *J. Polymer Sci.* 1955, 18, 527-533.



15. Chiu, Y. S.; Keh, H. J. Sedimentation Velocity and Potential in a Concentrated Suspension of Charged Soft Spheres. *Colloids Surfaces A* 2014, 440, 185-196.
16. Ohshima, H. Sedimentation Potential and Velocity in a Concentrated Suspension of Soft Particles. *J. Colloid Interface Sci.* 2000, 229, 140-147.
17. Jiemvarangkula, P.; Zhang, W.; Lien, H.-L. Enhanced Transport of Polyelectrolyte Stabilized Nanoscale Zero-Valent Iron (nZVI) in Porous Media. *Chem. Eng. J.* 2011, 170, 482-491.
18. Lee, S. Y.; Yalcin, S. E.; Joo, S. W.; Sharma, A.; Baysal, O.; Qian, S. The Effect of Axial Concentration Gradient on Electrophoretic Motion of a Charged Spherical Particle in a Nanopore. *Microgravity Sci. Technol.* 2010, 22, 329-338.
19. Prakash, J. Hydrodynamic mobility of a porous spherical particle with variable permeability in a spherical cavity. *Microsystem Technol.* 2020, 26, 2601-2614.
20. Lee, T. C.; Keh, H. J. Slow Motion of a Spherical Particle in a Spherical Cavity with Slip Surfaces. *Int. J. Eng. Sci.* 2013, 69, 1-15.
21. Chen, S.B.; Ye, X. Boundary effect on slow motion of a composite sphere perpendicular to two parallel impermeable plates. *Chem. Eng. Sci.* 2000, 55, 2441-2453.
22. Kim, S.; Karrila, S. J. *Microhydrodynamics: Principles and Selected Applications*; Dover: Mineola, N. Y., 2005.



23. Happel, J.; Brenner, H. Low Reynolds Number Hydrodynamics; Nijhoff: Dordrecht, The Netherlands, 1983.
24. Pujar, N. S.; Zydny, A. L. Boundary Effects on the Sedimentation and Hindered Diffusion of Charged Particles. *AIChE J.* 1996, 42, 2101-2111.
25. Lee, E.; Yen, C.-B.; Hsu, J.-P. Sedimentation of a Nonconducting Sphere in a Spherical Cavity. *J. Phys. Chem. B* 2000, 104, 6815-6820.
26. Keh, H. J.; Cheng, T. F. Sedimentation of a Charged Colloidal Sphere in a Charged Cavity. *J. Chem. Phys.* 2011, 135, 214706-1-10.
27. Chang, Y. J.; Keh, H. J. Sedimentation of a Charged Porous Particle in a Charged Cavity. *J. Phys. Chem. B* 2013, 117, 12319-12327.
28. Masliyah, J. H.; Polikar, M. Terminal Velocity of Porous Spheres. *Can. J. Chem. Eng.* 1980, 58, 299-302.
29. Matsumoto, K.; Suganuma, A. Settling Velocity of a Permeable Model Floc. *Chem. Eng. Sci.* 1977, 32, 445-447.
30. Aoyanagi, O.; Muramatsu, N.; Ohshima, H.; Kondo, T. Electrophoretic Behavior of PolyA-Graft-PolyB-Type Microcapsules. *J. Colloid Interface Sci.* 1994, 162, 222-226.
31. Morita, K.; Muramatsu, N.; Ohshima, H.; Kondo, T. Electrophoretic Behavior of Rat Lymphocyte Subpopulations. *J. Colloid Interface Sci.* 1991, 147, 457-461.



32. Kawahata, S.; Ohshima, H.; Muramatsu, N.; Kondo, T. Charge Distribution in the Surface Region of Human Erythrocytes as Estimated from Electrophoretic Mobility Data. *J. Colloid Interface Sci.* 1990, 138, 182-186.
33. Ahualli, S.; Jimenez, M. L.; Carrique, F.; Delgado, A. V. AC Electrokinetics of Concentrated Suspensions of Soft Particles. *Langmuir* 2009, 25, 1986-1997.
34. Lopez-Garcia, J. J.; Grosse, C.; Horno, J. Numerical Calculation of the Electrophoretic Mobility of Concentrated Suspensions of Soft Particles. *J. Colloid Interface Sci.* 2006, 301, 651-659.
35. Koplik, J.; Levine, H.; Zee, A. Velocity Renormalization in the Brinkman Equation. *Phys. Fluids* 1983, 26, 2864-2870.
36. Neale, G.; Epstein, N.; Nader, W. Creeping Flow Relative to Permeable Spheres. *Chem. Eng. Sci.* 1973, 28, 1865-1874.
37. Chen, W.J.; Keh, H.J. Electrophoresis of a charged soft particle in a charged cavity with arbitrary double-layer thickness. *J. Phys. Chem. B* 2013, 117, 9757-9767.
38. Makino, K.; Yamamoto, S.; Fujimoto, K.; Kawaguchi, H.; Ohshima, H. Surface Structure of Latex Particles Covered with Temperature-Sensitive Hydrogel Layers. *J. Colloid Interface Sci.* 1994, 166, 251-258.



39. Blaakmeer, J.; Bohmer, M. R.; Cohen Stuart, M. A.; Fleer, G. J. Adsorption of Weak Polyelectrolytes on Highly Charged Sur-faces. Poly(Acrylic Acid) on Polystyrene Latex with Strong Cationic Groups. *Macromolecules* 1990, 23, 2301-2309.

40. Keh, H. J.; Chou, J. Creeping Motions of a Composite Sphere in a Concentric Spherical Cavity. *Chem. Eng. Sci.* 2004, 59, 407-415.

Appendix A

Some Functions in Equations (15)-(17)



.In Equation (15),

$$F_{00r}(r) = C_{001} + [C_{002} + C_{003}\alpha(\lambda r) + C_{004}\beta(\lambda r)]\left(\frac{a}{r}\right)^3 \quad \text{for } r_0 < r < a, \quad (\text{A1a})$$

$$F_{00r}(r) = C_{005} + C_{006}\frac{a}{r} + C_{007}\left(\frac{a}{r}\right)^3 + C_{008}\left(\frac{r}{a}\right)^2 \quad \text{for } a < r < b, \quad (\text{A1b})$$

$$F_{p00}(r) = \left[\frac{1}{2}C_{002}\left(\frac{a}{r}\right)^2 - C_{001}\frac{r}{a}\right](\lambda a)^2 \quad \text{for } r_0 < r < a, \quad (\text{A2a})$$

$$F_{p00}(r) = C_{006}\left(\frac{a}{r}\right)^2 + 10C_{008}\frac{r}{a} \quad \text{for } a < r < b; \quad (\text{A2b})$$

$$\begin{aligned} F_{ijr}(r) = & C_{ij1} + [C_{ij2} + C_{ij3}\alpha(\lambda r) + C_{ij4}\beta(\lambda r)]\left(\frac{a}{r}\right)^3 + \frac{2}{3(\lambda a)^2}\{J_{ij}^{(0)}(r_0, r) \\ & - \left(\frac{a}{r}\right)^3 J_{ij}^{(3)}(r_0, r) + \frac{3\alpha(\lambda r)}{(\lambda r)^3} J_{ij}^{\beta}(r_0, r) - \frac{3\beta(\lambda r)}{(\lambda r)^3} J_{ij}^{\alpha}(r_0, r)\} \quad \text{for } r_0 < r < a, \end{aligned} \quad (\text{A3a})$$

$$\begin{aligned} F_{ijr}(r) = & C_{ij5} + \frac{1}{3}J_{ij}^{(2)}(a, r) + \frac{a}{r}[C_{ij6} - \frac{1}{3}J_{ij}^{(3)}(a, r)] \\ & + \left(\frac{a}{r}\right)^3[C_{ij7} + \frac{1}{15}J_{ij}^{(5)}(a, r)] + \left(\frac{r}{a}\right)^2[C_{ij8} - \frac{1}{15}J_{ij}^{(0)}(a, r)] \quad \text{for } a < r < b, \end{aligned} \quad (\text{A3b})$$

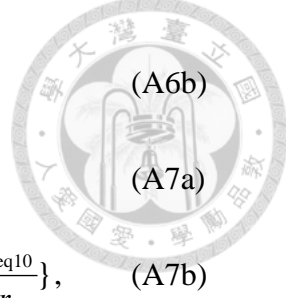
$$\begin{aligned} F_{prij}(r) = & (\lambda a)^2\left[\frac{1}{2}C_{ij2}\left(\frac{a}{r}\right)^2 - C_{ij1}\frac{r}{a}\right] - \frac{1}{3}\left(\frac{a}{r}\right)^2 J_{ij}^{(3)}(r_0, r) - \frac{2r}{3a} J_{ij}^{(0)}(r_0, r) \\ & \quad \text{for } r_0 < r < a, \end{aligned} \quad (\text{A4a})$$

$$F_{prij}(r) = \left(\frac{a}{r}\right)^2[C_{ij6} - \frac{1}{3}J_{ij}^{(3)}(a, r)] + \frac{r}{a}[10C_{ij8} - \frac{2}{3}J_{ij}^{(0)}(a, r)] \quad \text{for } a < r < b, \quad (\text{A4b})$$

where (i, j) equal (0,2), (1,1), and (2,0),

$$J_{ij}^{(n)}(r_1, r_2) = \int_{r_1}^{r_2} \left(\frac{r}{a}\right)^n G_{ij}(r) dr, \quad (\text{A5})$$

$$J_{ij}^{\alpha}(r_1, r_2) = \int_{r_1}^{r_2} \alpha(\lambda r) G_{ij}(r) dr, \quad (\text{A6a})$$



(A6b)

(A7a)

$$J_{ij}^\beta(r_1, r_2) = \int_{r_1}^{r_2} \beta(\lambda r) G_{ij}(r) dr,$$

$$G_{02}(r) = \frac{\varepsilon(\kappa a)^2}{2\eta r} [F_{01+}(r) - F_{01-}(r)] \frac{d\psi_{eq01}}{dr},$$

$$G_{11}(r) = \frac{\varepsilon(\kappa a)^2}{2\eta r} \{ [F_{10+}(r) - F_{10-}(r)] \frac{d\psi_{eq01}}{dr} + [F_{01+}(r) - F_{01-}(r)] \frac{d\psi_{eq10}}{dr} \}, \quad (A7b)$$

$$G_{20}(r) = \frac{\varepsilon(\kappa a)^2}{2\eta r} [F_{10+}(r) - F_{10-}(r)] \frac{d\psi_{eq10}}{dr}, \quad (A7c)$$

$$\alpha(x) = x \cosh x - \sinh x, \quad (A8a)$$

$$\beta(x) = x \sinh x - \cosh x, \quad (A8b)$$

and expressions of the coefficients C_{00n} , C_{02n} , C_{11n} , and C_{20n} with $n=1, 2, \dots$, and 8 are lengthy and given in Equations (A15) and (A16).

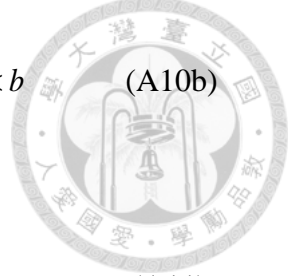
In Equations (16) and (17),

$$F_{ij\pm}(r) = \pm \frac{1}{3D_\pm(b^3 - r_0^3)} \{ a^3 r [2 + (\frac{r_0}{r})^3] [G_3(a, b) + G_3(r_0, a)] + b^3 r [1 + \frac{1}{2} (\frac{r_0}{r})^3] [G_0(a, b) + G_0(r_0, a)] + (b^3 - r_0^3) [a^3 r^{-2} G_3(r_0, r) - r G_0(r_0, r)] \} \quad \text{for } r_0 < r < a \quad (A9a)$$

$$F_{ij\pm}(r) = \pm \frac{1}{3D_\pm(b^3 - r_0^3)} [a^3 r \{ [2 + (\frac{b}{r})^3] G_3(r_0, a) + [2 + (\frac{r_0}{r})^3] G_3(a, b) \} + r \{ r_0^3 [1 + \frac{1}{2} (\frac{b}{r})^3] G_0(r_0, a) + b^3 [1 + \frac{1}{2} (\frac{r_0}{r})^3] G_0(a, b) \} + (b^3 - r_0^3) \{ a^3 r^{-2} G_3(a, r) - r G_0(a, r) \}] \quad \text{for } a < r < b \quad (A9b)$$

$$F_{\psi ij}(r) = \frac{1}{2\kappa r^2} [\alpha(\kappa r) B_{\psi ij}(r_0, r) - \beta(\kappa r) A_{\psi ij}(r_0, r)] + \frac{1}{2W\kappa r^2} \{ \Omega_4 \beta(\kappa r) [e^{\kappa r_0} \Omega_1 A_{\psi ij}(r_0, b) + e^{\kappa(b+r_0)} \Omega_2 \{ A_{\psi ij}(r_0, b) - B_{\psi ij}(r_0, b) \}] - [\alpha(\kappa r) \Omega_1 A_{\psi ij}(r_0, b) - e^{\kappa b} \Omega_2 \Omega_5 \{ A_{\psi ij}(r_0, b) - B_{\psi ij}(r_0, b) \}] \} \quad \text{for } r_0 < r < a \quad (A10a)$$

$$F_{\psi ij}(r) = \frac{1}{2\kappa r^2} [\alpha(\kappa r) B_{\psi ij}(a, r) - \beta(\kappa r) A_{\psi ij}(a, r)] - \frac{1}{2W\kappa r^2} \{ \Omega_4 \beta(\kappa r) [e^{\kappa r_0} \Omega_1 A_{\psi ij}(a, b) - e^{\kappa(b+r_0)} \Omega_2 \{ A_{\psi ij}(a, b) - B_{\psi ij}(r_0, r) \}] + [e^{\kappa b} \Omega_2 \Omega_5 A_{\psi ij}(r_0, a)] + \alpha(\kappa r) [e^{\kappa b} \Omega_2 \Omega_3 B_{\psi ij}(a, b) + e^{\kappa r_0} \Omega_1 \Omega_4 B_{\psi ij}(r_0, a)] \} \quad (A10b)$$



$$-\mathrm{e}^{\kappa(b+r_0)}\Omega_2\Omega_4B_{\psi ij}(r_0,b)+\Omega_5(\Omega_1-\mathrm{e}^{\kappa b}\Omega_2)A_{\psi ij}(r_0,b)]\} \text{ for } a < r < b \quad (\text{A10b})$$

where (i, j) equal $(0,1)$ and $(1,0)$,

$$G_n(r_1, r_2) = \int_{r_1}^{r_2} \left(\frac{r}{a}\right)^n \frac{d\psi_{eqij}}{dr} F_{00r}(r) dr, \quad (\text{A11})$$

$$A_{\psi ij}(r_1, r_2) = \int_{r_1}^{r_2} \alpha(\kappa r)[F_{ij+}(r) - F_{ij-}(r)] dr, \quad (\text{A12a})$$

$$B_{\psi ij}(r_1, r_2) = \int_{r_1}^{r_2} \beta(\kappa r)[F_{ij+}(r) - F_{ij-}(r)] dr, \quad (\text{A12b})$$

$$W = \mathrm{e}^{\kappa b}\Omega_2\Omega_3 - \mathrm{e}^{\kappa r_0}\Omega_1\Omega_4, \quad (\text{A13})$$

$$\Omega_1 = 2 + \kappa b(2 + \kappa b), \quad (\text{A14a})$$

$$\Omega_2 = 2\alpha(\kappa b) - (\kappa b)^2 \sinh(\kappa b), \quad (\text{A14b})$$

$$\Omega_3 = 2 + \kappa r_0(2 + \kappa r_0), \quad (\text{A14c})$$

$$\Omega_4 = 2\alpha(\kappa r_0) - (\kappa r_0)^2 \sinh(\kappa r_0), \quad (\text{A14d})$$

$$\Omega_5 = \Omega_3 - \mathrm{e}^{\kappa r_0}\Omega_4. \quad (\text{A14e})$$

In Equations (A1)-(A4),

$$\begin{aligned} C_{001} = & \frac{1}{N} 6b\{r_0\lambda(3a^5\lambda^2 + 2b^5\lambda^2 - 5a^3(18 + b^2\lambda^2)) + 2a\lambda \\ & (45a^3 + (6a^5 - 5a^3b^2 - b^5)\lambda^2)\cosh((a - r_0)\lambda) + \\ & 2(-21a^5\lambda^2 + b^5\lambda^2 + 5a^3(-9 + b^2\lambda^2))\sinh((a - r_0)\lambda)\} \end{aligned} \quad (\text{A15a})$$

$$\begin{aligned} C_{002} = & \frac{1}{\lambda^2 a^3 N} [12br_0(a^3(3a^5 - 5a^3b^2 + 2b^5)\lambda^5 + \lambda \cosh(\lambda(a - r_0))) \\ & (-135a^3(a - r_0) + a(-6a^5 + 5a^3b^2 + b^5)\lambda^4 r_0^2 - 3\lambda^2(a - r_0) \\ & (6a^5 - 5a^3b^2 - b^5 - 15a^4r_0)) + \sinh(\lambda(a - r_0))(135a^3 + \lambda^4 r_0(-18a^6 + \\ & 15a^4b^2 + 3ab^5 + 21a^5r_0 - 5a^3b^2r_0 - b^5r_0) + \\ & 3\lambda^2(21a^5 - b^5 - 45a^4r_0 - 5a^3(b^2 - 3r_0^2))))] \end{aligned} \quad (\text{A15b})$$



$$\begin{aligned}
C_{003} = & \frac{1}{a^3 \lambda^2 N} [6b(6(-21a^5 \lambda^2 + b^5 \lambda^2 + 5a^3(-9 + b^2 \lambda^2)) \cosh(a\lambda) r_0 + \\
& 6a\lambda(45a^3 + (6a^5 - 5a^3b^2 - b^5)\lambda^2) \sinh(a\lambda) r_0 + 3\lambda(3a^5 \lambda^2 + 2b^5 \lambda^2 - \\
& 5a^3(18 + b^2 \lambda^2)) \sinh(\lambda r_0) r_0^2 + \cosh(\lambda r_0)(270a^3 r_0 - (a - b)^2(3a^3 + 6a^2b + \\
& 4ab^2 + 2b^3)\lambda^4(2a^3 + r_0^3) + 3\lambda^2 r_0(-3a^5 - 2b^5 + 5a^3(b^2 + 6r_0^2))))]
\end{aligned} \tag{A15c}$$

$$\begin{aligned}
C_{004} = & \frac{1}{a^3 \lambda^2 N} [6b(3r_0(2a\lambda(-6a^5 \lambda^2 + b^5 \lambda^2 + 5a^3(-9 + b^2 \lambda^2)) \cosh(a\lambda) + \\
& 2(45a^3 + (21a^5 - 5a^3b^2 - b^5)\lambda^2) \sinh(a\lambda) + \lambda(-3a^5 \lambda^2 - 2b^5 \lambda^2 + \\
& 5a^3(18 + b^2 \lambda^2)) \cosh(\lambda r_0) r_0 + \sinh(\lambda r_0)(-270a^3 r_0 + (a - b)^2(3a^3 + \\
& 6a^2b + 4ab^2 + 2b^3)\lambda^4(2a^3 + r_0^3) + 3\lambda^2 r_0(3a^5 + 2b^5 - 5a^3(b^2 + 6r_0^2))))]
\end{aligned} \tag{A15d}$$

$$\begin{aligned}
C_{005} = & \frac{-b}{N} [6\lambda(180a^3 + (54a^5 - 5a^3b^2 - 4b^5)\lambda^2) r_0 + 3\sinh(\lambda(a - r_0)) \\
& (180a^3 + \lambda^2(144a^5 - 4b^5 + 45a^4 r_0 - 15a^2b^2 r_0 - 20a^3(b^2 + 9r_0^2)) + \\
& \lambda^4(30a^7 + 5a^3b^2 r_0^2 + 4b^5 r_0^2 + 15a^4 r_0^3 - 5a^2b^2 r_0^3 - a^5(10b^2 + 9r_0^2)) + \\
& \lambda \cosh(\lambda(a - r_0))(-540a^3(a + r_0) - (9a^5 - 5a^3b^2 - 4b^5)\lambda^4(2a^3 + r_0^3) - \\
& 3\lambda^2(84a^6 - 4ab^5 + 9a^5 r_0 - 4b^5 r_0 + 15a^2b^2 r_0^2 - 5a^4(4b^2 + 9r_0^2) + \\
& a^3(-5b^2 r_0 + 60r_0^3)))]
\end{aligned} \tag{A15e}$$

$$\begin{aligned}
C_{006} = & \frac{1}{aN} [6b(60a^6 \lambda^3 r_0 - \lambda \cosh(\lambda(a - r_0))\{135a^3(a - r_0)r_0 + a(a^5 - b^5)\lambda^4 \\
& (2a^3 + r_0^3) + 3\lambda^2(10a^7 + a^6 r_0 - ab^5 r_0 - 6a^5 r_0^2 + b^5 r_0^2 + 15a^4 r_0^3)\} + \\
& \sinh(\lambda(a - r_0))\{135a^3 r_0 + 3\lambda^2(10a^6 + 6a^5 r_0 - b^5 r_0 - 45a^4 r_0^2 + 15a^3 r_0^3) + \\
& \lambda^4(12a^8 - 2a^3b^5 - 3a^6 r_0^2 + 3ab^5 r_0^2 + 6a^5 r_0^3 - b^5 r_0^3)\}]
\end{aligned} \tag{A15f}$$

$$\begin{aligned}
C_{007} = & \frac{1}{aN} [2b^3(6a(-10a^3 + b^3)\lambda^3 r_0 + 3\sinh(\lambda(a - r_0))(-45ar_0 + \\
& \lambda^2(-10a^4 + 4ab^3 - 6a^3 r_0 + 3b^3 r_0 + 45a^2 r_0^2 - 15ar_0^3) + \lambda^4 \\
& (-4a^6 + a^4 r_0^2 - ab^3 r_0^2 + b^3 r_0^3 + 2a^3(b^3 - r_0^3))) + \lambda \cosh(\lambda(a - r_0)) \\
& \{135a(a - r_0)r_0 + a(a^3 - b^3)\lambda^4(2a^3 + r_0^3) + 3\lambda^2(10a^5 + a^4 r_0 - ab^3 r_0 \\
& - 6a^3 r_0^2 + 3b^3 r_0^2 + a^2(-4b^3 + 15r_0^3))\})]
\end{aligned} \tag{A15g}$$



$$C_{008} = \frac{-1}{N} [3a^2b\lambda^2(-6a^3\lambda r_0 + \lambda \cosh(\lambda(a - r_0))\{3(4a^4 + a^3r_0 - ab^2r_0 - 3a^2r_0^2 + b^2r_0^2) + a(a - b)(a + b)\lambda^2(2a^3 + r_0^3)\} + \sinh(\lambda(a - r_0))) \\ \{-12a^3 - 9a^2r_0 + 3b^2r_0 + \lambda^2(-6a^5 - 3ab^2r_0^2 - 3a^2r_0^3 + b^2r_0^3 + a^3(2b^2 + 3r_0^2)))\}] \quad (\text{A15h})$$

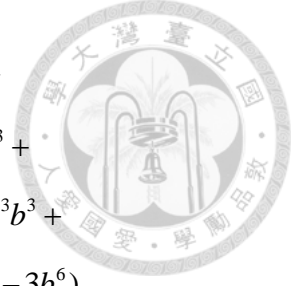
$$C_{ij1} = \frac{1}{3(\lambda a)^2 N} \{2(3r_0\lambda(-180a^3bL_1 + 2(2b^6L_1 + 5a^3b^3(L_1 + 3L_2) - 9a^5b(3L_1 + 5L_5) + 10a^6(2L_1 + 3L_7))\lambda^2 + a^2(2b^6(-L_2 + L_5) + 3ab^5(L_2 - L_7) + 3a^5b(L_5 - L_8) + 2a^6(-L_7 + L_8) + a^3b^3(-L_2 - 5L_5 + 5L_7 + L_8))\lambda^4) + 3r_0(180a^3L_3 + 180a^3(a - b)L_4\lambda + 3(a - b)^3(8a^2 + 9ab + 3b^2)L_3\lambda^2 + (a - b)^4(4a^2 + 7ab + 4b^2)L_4\lambda^3)\cosh(a\lambda) - a\lambda(-540a^3bL_1 + 6(2b^6L_1 + 5a^3b^3(4L_1 + 3L_2) - 3a^5b(14L_1 + 15L_5 + 10L_6) + 10a^6(2L_1 + 3(L_6 + L_7)))\lambda^2 + a^2(2b^6(4L_1 + 3(L_2 + L_5) + 2L_6) - 9ab^5(2L_1 + 2L_2 + L_6 + L_7) + 4a^6(2L_1 + L_6 + 6L_7 - 3L_8) - 9a^5b(2L_1 + 4L_5 + L_6 - L_8) + a^3b^3(20L_1 + 12L_2 + 30L_5 + 10L_6 - 15L_7 + 3L_8))\lambda^4)\cosh((a - r_0)\lambda) + 6L_3(20a^6\lambda^2 - 27a^5b\lambda^2 + 2b^6\lambda^2 + 5a^3b(-18 + b^2\lambda^2))\cosh(\lambda r_0) - 3r_0(180a^3L_4 + 180a^3(a - b)L_3\lambda + 3(a - b)^3(8a^2 + 9ab + 3b^2)L_4\lambda^2 + (a - b)^4(4a^2 + 7ab + 4b^2)L_3\lambda^3)\sinh(a\lambda) + 3(-180a^3bL_1 + 2(2b^6L_1 + 5a^3b^3(4L_1 + 3L_2) - 9a^5b(8L_2 + 5L_5) + 10a^6(2L_1 + 3(L_6 + L_7)))\lambda^2 + a^2(2b^6(-L_2 + L_5) - 3ab^5(2L_1 + 2L_2 + L_6 + L_7) + 4a^6(4L_1 + 2L_6 + 7L_7 - L_8) - 3a^5b(10L_1 + 14L_5 + 5L_6 + L_8) + a^3b^3(20L_1 + 14L_2 + 5(2(L_5 + L_6) + L_7) + L_8)\lambda^4)\sinh((a - r_0)\lambda) - 6L_4(20a^6\lambda^2 - 27a^5b\lambda^2 + 2b^6\lambda^2 + 5a^3b(-18 + b^2\lambda^2))\sinh(\lambda r_0))\} \quad (\text{A16a})$$



$$\begin{aligned}
C_{ij2} = & (2r_0(-90a^6bL_6\lambda^3 + 60a^4b^3L_6\lambda^3 + 6a^3b^3(a^3 + b^3)L_2\lambda^5 - 18a^8bL_5\lambda^5 - \\
& 12a^3b^6L_5\lambda^5 + 4a^9L_6\lambda^5 - 3a^8bL_6\lambda^5 - 5a^6b^3L_6\lambda^5 + 6a^4b^5L_6\lambda^5 - 2a^3b^6L_6\lambda^5 + \\
& 12a^9L_7\lambda^5 - 15a^6b^3L_7\lambda^5 + 18a^4b^5L_7\lambda^5 + 9a^8bL_8\lambda^5 - 6a^6b^3L_8\lambda^5 + 2L_1\lambda^3 \\
& (-6b(3a^6 + 2ab^5) + a^3(4a^6 - 3a^5b - 5a^3b^3 + 6ab^5 - 2b^6)\lambda^2) + 6(15b(3a^3 - \\
& 2ab^2)L_3 + 15a^2(3a^2b - 2b^3)L_4\lambda + (4a^6 + 24a^5b - 20a^3b^3 + 6ab^5 + b^6)L_3\lambda^2 + \\
& a(4a^6 + 3a^5b - 10a^3b^3 + 6ab^5 - 3b^6)L_4\lambda^3)\cosh(\lambda a) - 6(15b(3a^3 - 2ab^2)L_4 + \\
& 15a^2(3a^2b - 2b^3)L_3\lambda + (4a^6 + 24a^5b - 20a^3b^3 + 6ab^5 + b^6)L_4\lambda^2 + a(4a^6 + \\
& 3a^5b - 10a^3b^3 + 6ab^5 - 3b^6)L_3\lambda^3)\sinh(\lambda a) - \frac{2}{N}(-6ab(3a^5 + 2b^5)\lambda^3 + a^3 \\
& (4a^6 - 3a^5b - 5a^3b^3 + 6ab^5 - 2b^6)\lambda^5 + \lambda(-45a(3a^2b - 2b^3)(a - r_0) + 3(-4a^7 + \\
& 24a^5br_0 - 20a^3b^3r_0 + b^6r_0 + 3ab^5(b + 2r_0) + a^6(-3b + 4r_0) + 5a^4(2b^3 - 3br_0^2) + \\
& a^2(-6b^5 + 10b^3r_0^2))\lambda^2 + a(-4a^6 - 3a^5b + 10a^3b^3 - 6ab^5 + 3b^6)r_0^2\lambda^4) \\
& \cosh((a - r_0)\lambda) + (45ab(3a^2 - 2b^2) + 3(4a^6 + 24a^5b + b^6 - 45a^4br_0 + 30a^2b^3r_0 + \\
& 5a^3b(-4b^2 + 3r_0^2) + 2a(3b^5 - 5b^3r_0^2))\lambda^2 + r_0(-3a(4a^6 + 3a^5b - 10a^3b^3 + 6ab^5 - \\
& 3b^6) + (4a^6 + 24a^5b - 20a^3b^3 + 6ab^5 + b^6)r_0)\lambda^4)\sinh((a - r_0)\lambda))(3N_2r_0 - 3r_0 \\
& (180a^3L_3 + 180a^3(a - b)L_4\lambda + 3(a - b)^3(8a^2 + 9ab + 3b^2)L_3\lambda^2 + (a - b)^4(4a^2 + \\
& 7ab + 4b^2)L_4\lambda^3)\cosh(a\lambda) + a\lambda(-540a^3bL_1 + 6(2b^6L_1 + 5a^3b^3(4L_1 + 3L_2) - 3a^5b \\
& (14L_1 + 15L_5 + 10L_6) + 10a^6(2L_1 + 3(L_6 + L_7)))\lambda^2 + a^2(2b^6(4L_1 + 3(L_2 + \\
& L_5) + 2L_6) - 9ab^5(2L_1 + 2L_2 + L_6 + L_7) + 4a^6(2L_1 + L_6 + 6L_7 - 3L_8) - \\
& 9a^5b(2L_1 + 4L_5 + L_6 - L_8) + a^3b^3(20L_1 + 12L_2 + 30L_5 + 10L_6 - 15L_7 + 3L_8))\lambda^4) \\
& \cosh((a - r_0)\lambda)a\lambda(-540a^3bL_1 + 6(2b^6L_1 + 5a^3b^3(4L_1 + 3L_2) - 3a^5b(14L_1 + \\
& 15L_5 + 10L_6) + 10a^6(2L_1 + 3(L_6 + L_7)))\lambda^2 - 6L_3(20a^6\lambda^2 - 27a^5b\lambda^2 + 2b^6\lambda^2 + 5a^3b \\
& (-18 + b^2\lambda^2))\cosh(\lambda r_0) - 3N_1\sinh((a - r_0)\lambda) + 6L_4(20a^6\lambda^2 - 27a^5b\lambda^2 + 2b^6\lambda^2 + \\
& 5a^3b(-18 + b^2\lambda^2))\sinh(\lambda r_0))) / (3a^5\lambda^4(30b(-3a^3 + 2ab^2)r_0\lambda + (4a^6 - 3a^5b - \\
& 5a^3b^3 + 6ab^5 - 2b^6)r_0\lambda^3 + 2a\lambda(45a^3b - 30ab^3 + (4a^6 + 3a^5b - 10a^3b^3 + 6ab^5 - \\
& 3b^6)\lambda^2)\cosh((a - r_0)\lambda) - 2(45a^3b - 30ab^3 + (4a^6 + 24a^5b - 20a^3b^3 + \\
& 6ab^5 + b^6)\lambda^2)\sinh((a - r_0)\lambda)))
\end{aligned} \tag{A16b}$$



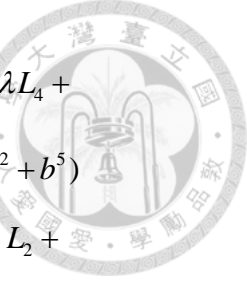
$$\begin{aligned}
C_{ij3} = & \frac{1}{(\lambda a)^5 N} \{ -2\lambda r_0 (-6(20a^6\lambda^2 - 27a^5b\lambda^2 + 2b^6\lambda^2 + 5a^3b(-18 + b^2\lambda^2))L_4 + \\
& a\lambda \sinh(a\lambda)(-540a^3bL_1 + 6\lambda^2(2b^6L_1 + 5a^3b^3(4L_1 + 3L_2) - 3a^5b(14L_1 + 15L_5) \\
& + 10L_6) + 10a^6(2L_1 + 3(L_6 + L_7))) + a^2\lambda^4(2b^6(4L_1 + 3(L_2 + L_5) + 2L_6) - \\
& 9ab^5(2L_1 + 2L_2 + L_6 + L_7) + 4a^6(2L_1 + L_6 + 6L_7 - 3L_8) - 9a^5b(2L_1 + 4L_5 + \\
& L_6 - L_8) + a^3b^3(20L_1 + 12L_2 + 30L_5 + 10L_6 - 15L_7 + 3L_8))) + 3N_2 \sinh(\lambda r_0)r_0) + \\
& 2\cosh(\lambda r_0)(540a^3b\lambda L_1r_0 + a^2(a-b)^2\lambda^7(2b^4(L_2 - L_5) + 6a^2b^2(-L_5 + L_7) + \\
& ab^3(L_2 - 4L_5 + 3L_7) + 2a^4(L_7 - L_8) - a^3b(3L_5 - 4L_7 + L_8))(2a^3 + r_0^3) + \lambda^5 \\
& (2a^3(20a^6L_6 + 2b^6(3L_2 + L_6) + 5a^3b^3(L_6 - 3L_7) + 9a^5b(-3L_6 + L_8)) + \\
& 3a^2(2b^6(L_2 - L_5) + 3ab^5(-L_2 + L_7) + a^3b^3(L_2 + 5L_5 - 5L_7 - L_8) + 2a^6(L_7 - L_8) + \\
& 3a^5b(-L_5 + L_8))r_0 - 2(2b^6L_1 + 5a^3b^3(L_1 + 3L_2) - 9a^5b(3L_1 + 5L_5) + \\
& 10a^6(2L_1 + 3L_7))r_0^3) - 6\lambda^3(2b^6L_1r_0 - 9a^5b(3L_1 + 5L_5)r_0 + 10a^6(3bL_6 + \\
& 2L_1r_0 + 3L_7r_0) + 5a^3br_0(b^2(L_1 + 3L_2) - 6L_1r_0^2)) + \sinh(a\lambda)(540a^3L_4(-b + r_0) - \\
& 540a^3\lambda L_3(a(b - r_0) + br_0) + (a-b)^4(4a^2 + 7ab + 4b^2)\lambda^5L_3(2a^3 + r_0^3) + \\
& 3(a-b)^3(8a^2 + 9ab + 3b^2)\lambda^4L_4(2a^3 + r_0^3) + 3\lambda^2L_4(4(10a^6 - 36a^5b + \\
& 10a^3b^3 + b^6) + 3(a-b)^3(8a^2 + 9ab + 3b^2)r_0 + 60a^3r_0^3) + 3\lambda^3L_3(4a(10a^6 - \\
& 21a^5b + 10a^3b^3 + b^6) + (a-b)^4(4a^2 + 7ab + 4b^2)r_0 + 60a^3(a-b)r_0^3)) - \\
& 2\cosh(a\lambda)(-3\lambda(N_1 + r_0)(180a^3L_3 + 180a^3(a-b)L4\lambda + 3(a-b)^3(8a^2 + 9ab + \\
& 3b^2)L_3\lambda^2 + (a-b)^4(4a^2 + 7ab + 4b^2)L_4\lambda^3)\sinh(\lambda r_0)r_0 + \cosh(\lambda r_0)(540a^3L_3 \\
& (-b + r_0) - 540a^3\lambda L_4(a(b - r_0) + br_0) + 3(a-b)^3(8a^2 + 9ab + 3b^2)\lambda^4L_3(2a^3 + r_0^3) \\
& + (a-b)^4(4a^2 + 7ab + 4b^2)\lambda^5L_4(2a^3 + r_0^3) + 3\lambda^2L_3(4(10a^6 - 36a^5b + 10a^3b^3 + \\
& b^6) + 3(a-b)^3(8a^2 + 9ab + 3b^2)r_0 + 60a^3r_0^3) + 3\lambda^3L_4(4a(10a^6 - 21a^5b + \\
& 10a^3b^3 + b^6) + (a-b)^4(4a^2 + 7ab + 4b^2)r_0 + 60a^3(a-b)r_0^3)))) \} \quad (\text{A16c})
\end{aligned}$$



$$\begin{aligned}
C_{ij4} = & \{2(\sinh(\lambda r_0)(-6\sinh(a\lambda)(15a^2(3a^2b-2b^3)\lambda L_3 + a(4a^6+3a^5b- \\
& 10a^3b^3+6ab^5-3b^6)\lambda^3 L_3 + 15b(3a^3-2ab^2)L_4 + (4a^6+24a^5b-20a^3b^3+ \\
& 6ab^5+b^6)\lambda^2 L_4) + 6\cosh(a\lambda)(15b(3a^3-2ab^2)L_3 + (4a^6+24a^5b-20a^3b^3+ \\
& 6ab^5+b^6)\lambda^2 L_3 + 15a^2(3a^2b-2b^3)\lambda L_4 + a(4a^6+3a^5b-10a^3b^3+6ab^5-3b^6) \\
& \lambda^3 L_4) - 6ab\lambda^3(4b^5L_1-10a^3b^2L_6+3a^5(2L_1+5L_6)) + a^3\lambda^5(-2b^6(2L_1-3L_2+ \\
& 6L_5+L_6)+4a^6(2L_1+L_6+3L_7)+6ab^5(2L_1+L_6+3L_7)-3a^5b(2L_1+6L_5+ \\
& L_6-3L_8)-a^3b^3(10L_1-6L_2+5L_6+15L_7+6L_8))) - \frac{1}{N}\lambda(-3N_1\sinh(\lambda(a-r_0))- \\
& 6(20a^6\lambda^2-27a^5b\lambda^2+2b^6\lambda^2+5a^3b(-18+b^2\lambda^2))\cosh(\lambda r_0)L_3 + 6(20a^6\lambda^2- \\
& 27a^5b\lambda^2+2b^6\lambda^2+5a^3b(-18+b^2\lambda^2))\sinh(\lambda r_0)L_4 + a\lambda\cosh(\lambda(a-r_0)) \\
& (-540a^3bL_1+6\lambda^2(2b^6L_1+5a^3b^3(4L_1+3L_2)-3a^5b(14L_1+15L_5+10L_6))+ \\
& 10a^6(2L_1+3(L_6+L_7)))+a^2\lambda^4[2b^6(4L_1+3(L_2+L_5)+2L_6)-9ab^5(2L_1+ \\
& 2L_2+L_6+L_7)+4a^6(2L_1+L_6+6L_7-3L_8)-9a^5b(2L_1+4L_5+L_6-L_8)+ \\
& a^3b^3(20L_1+12L_2+30L_5+10L_6-15L_7+3L_8)]) + 3N_2r_0 - 3\cosh(a\lambda) \\
& (180a^3L_3+3(a-b)^3(8a^2+9ab+3b^2)\lambda^2L_3+180a^3(a-b)\lambda L_4+(a-b)^4 \\
& (4a^2+7ab+4b^2)\lambda^3L_4)r_0) (-6a\lambda(45a^3b-30ab^3+(4a^6+3a^5b-10a^3b^3+ \\
& 6ab^5-3b^6)\lambda^2)\cosh(a\lambda)r_0 + 6(45a^3b-30ab^3+(4a^6+24a^5b-20a^3b^3+ \\
& 6ab^5+b^6)\lambda^2)\sinh(a\lambda)r_0 - 3\lambda(-90a^3b+60ab^3+(4a^6-3a^5b-5a^3b^3+ \\
& 6ab^5-2b^6)\lambda^2)\cosh(\lambda r_0)r_0^2 + \sinh(\lambda r_0)(90b(-3a^3+2ab^2)r_0+(a-b)^2 \\
& (4a^4+5a^3b+6a^2b^2+2ab^3-2b^4)\lambda^4(2a^3+r_0^3)-3\lambda^2(4a^6(3b-r_0)+3a^5br_0+ \\
& 2b^6r_0+5a^3br_0(b^2+6r_0^2)+a(8b^6-6b^5r_0-20b^3r_0^3))))\} / (3a^5\lambda^5(2a\lambda(45a^3b- \\
& 30ab^3+(4a^6+3a^5b-10a^3b^3+6ab^5-3b^6)\lambda^2)\cosh(\lambda(a-r_0))-2(45a^3b- \\
& 30ab^3+(4a^6+24a^5b-20a^3b^3+6ab^5+b^6)\lambda^2)\sinh(\lambda(a-r_0))+ \\
& 30b(-3a^3+2ab^2)\lambda r_0+(4a^6-3a^5b-5a^3b^3+6ab^5-2b^6)\lambda^3r_0)) \quad (A16d)
\end{aligned}$$



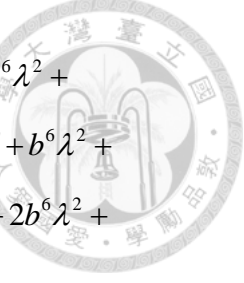
$$\begin{aligned}
C_{ij5} = & -\frac{1}{9a^2\lambda^5}\left\{-\frac{1}{3a^5b+2b^6}(3a^5b^3\lambda^5L_2-3\sinh(a\lambda)(a\lambda(4a^5\lambda^2+6b^5\lambda^2-5b^3\right. \\
& \left.(6+a^2\lambda^2))L_3+(4a^5\lambda^2+6b^5\lambda^2-15b^3(2+a^2\lambda^2))L_4)+3\cosh(a\lambda)((4a^5\lambda^2+\right. \\
& \left.6b^5\lambda^2-15b^3(2+a^2\lambda^2))L_3+a\lambda(4a^5\lambda^2+6b^5\lambda^2-5b^3(6+a^2\lambda^2))L_4)+a^2\lambda^3\right. \\
& \left.(2a(2a^5+3b^5)\lambda^2L_1-3b(3a^5+2b^5)\lambda^2L_5+a(30b^3+(2a^5+3b^5)\lambda^2)L_6+3a(2a^5+\right. \\
& \left.3b^5)\lambda^2L_7-3a^3b^3\lambda^2L_8))+(-6\sinh(a\lambda)(aN_3\lambda L_3+N_4L_4)+6\cosh(a\lambda)(N_4L_3+\right. \\
& \left.aN_3\lambda L_4)+a\lambda^3(2(-6b(3a^5+2b^5)+a^2(4a^6-3a^5b-5a^3b^3+6ab^5-2b^6)\lambda^2)L_1+\right. \\
& \left.6a^2b^3(a^3+b^3)\lambda^2L_2+a^2(-6b(3a^5+2b^5)\lambda^2L_5+(-90a^3b+60ab^3+(4a^6-3a^5b-\right. \\
& \left.5a^3b^3+6ab^5-2b^6)\lambda^2)L_6+3a(4a^5-5a^2b^3+6b^5)\lambda^2L_7+3a^3(3a^2b-2b^3)\lambda^2L_8)))\right. \\
& \left.(a\lambda(4a^5\lambda^2+6b^5\lambda^2-5b^3(6+a^2\lambda^2))\cosh(\lambda(a-r_0))+(30b^3+(-4a^5+15a^2b^3-\right. \\
& \left.6b^5)\lambda^2)\sinh(\lambda(a-r_0))+30b^3\lambda r_0+(2a^5+3b^5)\lambda^3r_0)\right)/\left(b(3a^5+2b^5)(2aN_3\lambda\right. \\
& \left.\cosh(\lambda(a-r_0))-2N_4\sinh(\lambda(a-r_0))+30b(-3a^3+2ab^2)\lambda r_0+(4a^6-3a^5b-\right. \\
& \left.5a^3b^3+6ab^5-2b^6)\lambda^3r_0)\right)+(\lambda^3(aN_5\lambda\cosh(\lambda(a-r_0))-3N_1\sinh(\lambda(a-r_0))-\right. \\
& \left.6(20a^6\lambda^2-27a^5b\lambda^2+2b^6\lambda^2+5a^3b(-18+b^2\lambda^2))\cosh(\lambda r_0)L_3+6(20a^6\lambda^2-\right. \\
& \left.27a^5b\lambda^2+2b^6\lambda^2+5a^3b(-18+b^2\lambda^2))\sinh(\lambda r_0)L_4+3N_2r_0-3\cosh(a\lambda)(180a^3L_3+\right. \\
& \left.3(a-b)^3(8a^2+9ab+3b^2)\lambda^2L_3+180a^3(a-b)\lambda L_4+(a-b)^4(4a^2+7ab+4b^2)\right. \\
& \left.\lambda^3L_4)r_0)(720ab^3\lambda r_0-6a(44a^5-35a^2b^3+6b^5)\lambda^3r_0+\lambda\cosh(\lambda(a-r_0))(180a\right. \\
& \left.(-2ab^3+3a^3r_0-2b^3r_0-3a^2r_0^2)+a(8a^5-5a^2b^3-3b^5)\lambda^4(2a^3+r_0^3)+3\lambda^2\right. \\
& \left.(8a^2(7a^5-5a^2b^3+3b^5)+a(8a^5-5a^2b^3-3b^5)r_0-3(12a^5-5a^2b^3+3b^5)r_0^2+\right. \\
& \left.20a(3a^3-2b^3)r_0^3))-3\sinh(\lambda(a-r_0))(60a(-2b^3+3a^2r_0)+\lambda^4(24a^8-\right. \\
& \left.10a^5b^3+6a^3b^5+a(-8a^5+5a^2b^3+3b^5)r_0^2+(12a^5-5a^2b^3+3b^5)r_0^3)+\lambda^2\right. \\
& \left.(56a^6+36a^5r_0-15a^2b^3r_0+9b^5r_0-180a^4r_0^2+24a(b^5+5b^3r_0^2)+a^3\right. \\
& \left.(-80b^3+60r_0^3))))/(N(2aN_3\lambda\cosh(\lambda(a-r_0))-2N_4\sinh(\lambda(a-r_0))+\right. \\
& \left.30b(-3a^3+2ab^2)\lambda r_0+(4a^6-3a^5b-5a^3b^3+6ab^5-2b^6)\lambda^3r_0))\right\} \quad (\text{A16e})
\end{aligned}$$



$$\begin{aligned}
C_{ij6} = & \frac{1}{3a^3N\lambda^2} \{ 36b \cosh(a\lambda)(-45a^3L_3 + (-21a^5 + 5a^3b^2 + b^5)\lambda^2 L_3 - 45a^4\lambda L_4 + \\
& a(-6a^5 + 5a^3b^2 + b^5)\lambda^3 L_4) r_0 + 6(-6b \sinh(a\lambda)(-45a^4\lambda L_3 + a(-6a^5 + 5a^3b^2 + b^5) \\
& \lambda^3 L_3 - 45a^3 L_4 + (-21a^5 + 5a^3b^2 + b^5)\lambda^2 L_4) - 90a^6b\lambda^3 L_6 + a^3\lambda^5(2b^6(2L_1 + L_2 + \\
& L_6) - 40a^6L_7 - 5a^3b^3(2L_1 + 4L_2 + L_6 + L_7) + 3a^5b(2L_1 + 20L_5 + L_6 + L_8)))r_0 - \\
& 6b \cosh(\lambda r_0)(-270a^3L_3r_0 - 270a^3\lambda L_4r_0^2 + 3(3a^5 - 5a^3b^2 + 2b^5)\lambda^3 L_4r_0^2 + (a-b)^2 \\
& (3a^3 + 6a^2b + 4ab^2 + 2b^3)\lambda^4 L_3(2a^3 + r_0^3) + 3\lambda^2 L_3r_0(3a^5 + 2b^5 - 5a^3(b^2 + 6r_0^2))) + \\
& 6b \sinh(\lambda r_0)(-270a^3L_4r_0 - 270a^3\lambda L_3r_0^2 + 3(3a^5 - 5a^3b^2 + 2b^5)\lambda^3 L_3r_0^2 + (a-b)^2 \\
& (3a^3 + 6a^2b + 4ab^2 + 2b^3)\lambda^4 L_4(2a^3 + r_0^3) + 3\lambda^2 L_4r_0(3a^5 + 2b^5 - 5a^3(b^2 + 6r_0^2))) + \\
& \lambda \cosh(\lambda(a - r_0))(-1620a^3bL_1(a - r_0)r_0 + a^3(a - b)\lambda^6(2b^5(L_2 - 3L_5) + 4a^5L_7 + \\
& a^2b^3(2L_2 - 6L_5 + 9L_7) + ab^4(2L_2 - 6L_5 + 9L_7) + a^4b(-6L_5 + 4L_7 - 3L_8) + \\
& a^3b^2(-6L_5 + 4L_7 - 3L_8))(2a^3 + r_0^3) + 18\lambda^2(2ab^6L_1r_0 - 2b^6L_1r_0^2 - 5a^3b^3(2L_1 + \\
& 3L_2)r_0^2 + 3a^5b(14L_1 + 15L_5)r_0^2 + 30a^7(bL_6 + L_7r_0) - 3a^6r_0(4bL_1 + 15bL_5 + \\
& 10L_7r_0) + 5a^4br_0(b^2(2L_1 + 3L_2) - 6L_1r_0^2)) + 3a\lambda^4(40a^9L_7 + 6ab^6(L_2 - L_5)r_0^2 - \\
& 3a^4b^3(4L_2 + 5L_7 + L_8)r_0^2 + 4b^6L_1r_0^3 + 4a^8(-3b(5L_5 - 2L_6 + L_8) + L_7r_0) - 3a^7r_0 \\
& (2bL_5 + bL_8 + 8L_7r_0) + a^2b^5r_0(-2bL_2 + 6bL_5 + 9L_7r_0) + a^5br_0(b^2(2L_2 + 5L_7 + \\
& 3L_8) - 6(4L_1 + 15L_5)r_0^2) + a^3b^3(-4b^3(2L_2 + L_6) - 9b^2L_7r_0 + 10(2L_1 + 3L_2)r_0^3) + \\
& a^6(20b^3(L_2 - L_6 + L_7) + 9b(4L_5 + L_8)r_0^2 + 60L_7r_0^3)) - 3\sinh(\lambda(a - r_0)) \\
& (-540a^3bL_1r_0 + \lambda^4(4a^3(-b^6(2L_2 + L_6) + 10a^6L_7 + 5a^3b^3(L_2 - L_6 + L_7) - \\
& 3a^5b(5L_5 - 7L_6 + L_8)) + 3a^2(2b^6(-L_2 + L_5) + 8a^6L_7 - 3ab^5L_7 - 3a^5b(4L_5 + L_8) + \\
& a^3b^3(4L_2 + 5L_7 + L_8))r_0 - 6a(2b^6L_1 + 5a^3b^3(2L_1 + 3L_2) - 3a^5b(4L_1 + 15L_5) + \\
& 30a^6L_7)r_0^2 + 2(2b^6L_1 + 5a^3b^3(2L_1 + 3L_2) - 3a^5b(14L_1 + 15L_5) + 30a^6L_7)r_0^3) + \\
& 6\lambda^2(2b^6L_1r_0 - 3a^5b(14L_1 + 15L_5)r_0 + 90a^4bL_1r_0^2 + 30a^6(bL_6 + L_7r_0) + \\
& 5a^3br_0(b^2(2L_1 + 3L_2) - 6L_1r_0^2)) + a^2\lambda^6(16a^9L_7 - 6a^8b(4L_5 + L_8) - 4a^7L_7r_0^2 + \\
& 9a^2b^5L_7r_0^2 + 2b^6(-L_2 + L_5)r_0^3 - 3a^5b(4L_5 + L_8)r_0^3 + ab^5r_0^2(2bL_2 - 6bL_5 - \\
& 3L_7r_0) + a^4b^3(-6b^2L_7 - (2L_2 + 5L_7 + 3L_8)r_0^2) + a^6(2b^3(4L_2 + 5L_7 + L_8) + \\
& 3b(2L_5 + L_8)r_0^2 + 8L_7r_0^3) + a^3b^3(4b^3(-L_2 + L_5) + (4L_2 + 5L_7 + L_8)r_0^3))) \} \quad (A16f)
\end{aligned}$$



$$\begin{aligned}
C_{ij7} = & -\frac{2}{45a^5\lambda^5}\left\{\frac{1}{3a^5+2b^5}[30b^2(\sinh(a\lambda)(a^5\lambda^2(a\lambda L_3 + L_4) + b^3(6a\lambda L_3 + \right. \\
& \left.a^3\lambda^3L_3 + 6L_4 + 3a^2\lambda^2L_4)) + \cosh(a\lambda)(-a^5\lambda^2(L_3 + a\lambda L_4) - b^3(6L_3 + 3a^2\lambda^2L_3 + \right. \\
& \left.6a\lambda L_4 + a^3\lambda^3L_4))) + 60a^3b^5\lambda^3L_6 + a^5\lambda^5(6b^5L_2 - 5a^3b^2(2L_1 + L_6 + 3L_7) + \right. \\
& \left.9a^5L_8)] - (5b^2(-6\sinh(a\lambda)(15a^2(3a^2b - 2b^3)\lambda L_3 + a(4a^6 + 3a^5b - 10a^3b^3 + \right. \\
& \left.6ab^5 - 3b^6)\lambda^3L_3 + 15b(3a^3 - 2ab^2)L_4 + (4a^6 + 24a^5b - 20a^3b^3 + 6ab^5 + b^6)\lambda^2L_4) + \right. \\
& \left.6\cosh(a\lambda)(15b(3a^3 - 2ab^2)L_3 + (4a^6 + 24a^5b - 20a^3b^3 + 6ab^5 + b^6)\lambda^2L_3 + \right. \\
& \left.15a^2(3a^2b - 2b^3)\lambda L_4 + a(4a^6 + 3a^5b - 10a^3b^3 + 6ab^5 - 3b^6)\lambda^3L_4) - 6ab\lambda^3 \right. \\
& \left.(4b^5L_1 - 10a^3b^2L_6 + 3a^5(2L_1 + 5L_6)) + a^3\lambda^5(-2b^6(2L_1 - 3L_2 + 6L_5 + L_6) + \right. \\
& \left.4a^6(2L_1 + L_6 + 3L_7) + 6ab^5(2L_1 + L_6 + 3L_7) - 3a^5b(2L_1 + 6L_5 + L_6 - 3L_8) - \right. \\
& \left.a^3b^3(10L_1 - 6L_2 + 5L_6 + 15L_7 + 6L_8))\right)(2a\lambda(6b^3 + a^2(a^3 + b^3)\lambda^2)\cosh(\lambda(a - r_0)) - \right. \\
& \left.2(6b^3 + a^2(a^3 + 3b^3)\lambda^2)\sinh(\lambda(a - r_0)) - 12b^3\lambda r_0 + a^5\lambda^3r_0)\right)/((3a^5 + 2b^5)(-2a\lambda \right. \\
& \left.(4a^6\lambda^2 + 3a^5b\lambda^2 - 3b^6\lambda^2 + 6ab^3(-5 + b^2\lambda^2) - 5a^3b(-9 + 2b^2\lambda^2))\cosh(\lambda(a - r_0)) + \right. \\
& \left.2(4a^6\lambda^2 + 24a^5b\lambda^2 + b^6\lambda^2 + 6ab^3(-5 + b^2\lambda^2) - 5a^3b(-9 + 4b^2\lambda^2))\sinh(\lambda(a - r_0)) + \right. \\
& \left.\lambda(-4a^6\lambda^2 + 3a^5b\lambda^2 + 2b^6\lambda^2 - 6ab^3(10 + b^2\lambda^2) + 5a^3b(18 + b^2\lambda^2)r_0)\right) + \\
& (10ab^3\lambda^3(aN_5\lambda\cosh(\lambda(a - r_0)) - 3N_1\sinh(\lambda(a - r_0))) - 6(20a^6\lambda^2 - 27a^5b\lambda^2 \right. \\
& \left.+ 2b^6\lambda^2 + 5a^3b(-18 + b^2\lambda^2))\cosh(\lambda r_0)L_3 + 6(20a^6\lambda^2 - 27a^5b\lambda^2 + 2b^6\lambda^2 + \right. \\
& \left.5a^3b(-18 + b^2\lambda^2))\sinh(\lambda r_0)L_4 + 3N_2r_0 - 3\cosh(a\lambda)(180a^3L_3 + 3(a - b)^3 \right. \\
& \left.(8a^2 + 9ab + 3b^2)\lambda^2L_3 + 180a^3(a - b)\lambda L_4 + (a - b)^4(4a^2 + 7ab + 4b^2)\lambda^3L_4)r_0 \right) \\
& (\lambda\cosh(\lambda(a - r_0))(a^2(2a^3 - 3ab^2 + b^3)\lambda^4(2a^3 + r_0^3) + 9(2ab^2(4b - 9r_0) + 15a^3r_0 - \right. \\
& \left.15a^2r_0^2 + 2b^2r_0(4b + 9r_0)) + 3\lambda^2(14a^6 + 2a^5r_0 + 8b^3r_0^3 - 3ab^2r_0^2(b + 6r_0) + \right. \\
& \left.a^2b^2r_0(b + 9r_0) - 3a^4(4b^2 + 3r_0^2) + a^3(8b^3 - 3b^2r_0 + 15r_0^3))) - 3(48b^3\lambda r_0 + 2a^2 \right. \\
& \left.(11a^3 - 12ab^2 + 7b^3)\lambda^3r_0 + \sinh(\lambda(a - r_0))(6b^2(4b - 9r_0) + 45a^2r_0 + a\lambda^4 \right. \\
& \left.(2a^3(3a^3 - 3ab^2 + b^3) - a(2a^3 - 3ab^2 + b^3)r_0^2 + (3a^3 - 3ab^2 + b^3)r_0^3) + \lambda^2 \right. \\
& \left.(14a^5 + 9a^4r_0 - 6b^2r_0^2(4b + 3r_0) + 3ab^2r_0(b + 18r_0) - \right.
\end{aligned}$$



$$\begin{aligned}
& 3a^3(4b^2 + 15r_0^2) + a^2(16b^3 - 9b^2r_0 + 15r_0^3)))) / ((2a\lambda(4a^6\lambda^2 + 3a^5b\lambda^2 - 3b^6\lambda^2 + \\
& 6ab^3(-5 + b^2\lambda^2) - 5a^3b(-9 + 2b^2\lambda^2))\cosh(\lambda(a - r_0)) - 2(4a^6\lambda^2 + 24a^5b\lambda^2 + b^6\lambda^2 + \\
& 6ab^3(-5 + b^2\lambda^2) - 5a^3b(-9 + 4b^2\lambda^2))\sinh(\lambda(a - r_0)) + \lambda(4a^6\lambda^2 - 3a^5b\lambda^2 - 2b^6\lambda^2 + \\
& 6ab^3(10 + b^2\lambda^2) - 5a^3b(18 + b^2\lambda^2))r_0)(\lambda\cosh(\lambda(a - r_0))(120a^7\lambda^2 + 8a^9\lambda^4 - \\
& 18a^8b\lambda^4 - 90a^2b^3\lambda^2r_0^2 + 4a^6\lambda^2(-63b + 5b^3\lambda^2 + 3r_0 + \lambda^2r_0^3) - 9a^5\lambda^2r_0(8r_0 + \\
& b(3 + \lambda^2r_0^2)) + b^5\lambda^2r_0(27r_0 + 4b(3 + \lambda^2r_0^2)) - 3a^4(-40b^3\lambda^2 + 6b^5\lambda^4 - 45b \\
& (-4 + \lambda^2r_0^2) - 60r_0(3 + \lambda^2r_0^2)) + 3ab^5\lambda^2(4b - 3r_0(3 + \lambda^2r_0^2)) + 2a^3 \\
& (4b^6\lambda^4 - 270r_0^2 - 90br_0(3 + \lambda^2r_0^2) + 5b^3\lambda^2r_0(3 + \lambda^2r_0^2))) - 3(4\lambda(20a^6\lambda^2 - \\
& 27a^5b\lambda^2 + 2b^6\lambda^2 + 5a^3b(-18 + b^2\lambda^2))r_0 + \sinh(\lambda(a - r_0))(16a^8\lambda^4 - \\
& 30a^7b\lambda^4 + 9ab^5\lambda^4r_0^2 + 10a^2b^3\lambda^2r_0(3 + \lambda^2r_0^2) + a^6(40\lambda^2 - 4\lambda^4r_0^2) - \\
& b^5\lambda^2(-4b + 9r_0 + 4b\lambda^2r_0^2 + 3\lambda^2r_0^3) - 15a^4\lambda^2r_0(12r_0 + b(3 + \lambda^2r_0^2)) - \\
& 2a^3(3b^5\lambda^4 + 5b^3\lambda^2(-4 + \lambda^2r_0^2) - 90b(-1 + \lambda^2r_0^2) - 30r_0(3 + \lambda^2r_0^2)) + \\
& a^5\lambda^2(20b^3\lambda^2 + 9b(-16 + \lambda^2r_0^2) + 8r_0(3 + \lambda^2r_0^2))))\} \quad (\text{A16g})
\end{aligned}$$



$$\begin{aligned}
C_{ij8} = & \frac{1}{45\lambda^5} \left\{ \frac{1}{3a^5 + 2b^5} [6b^5\lambda^5 L_2 + 15\cosh(a\lambda)((18 + (9a^2 - 2b^2)\lambda^2)L_3 + \right. \\
& a\lambda(18 + (3a^2 - 2b^2)\lambda^2)L_4) - 15\sinh(a\lambda)(a\lambda(18 + (3a^2 - 2b^2)\lambda^2)L_3 + \\
& (18 + (9a^2 - 2b^2)\lambda^2)L_4) + 5a^3\lambda^3(-(18 + b^2\lambda^2)L_6 - b^2\lambda^2(2L_1 + 3L_7)) + \\
& 9a^5\lambda^5L_8] - (5(-6\sinh(a\lambda)(aN_3\lambda L_3 + N_4L_4) + 6\cosh(a\lambda)(N_4L_3 + aN_3\lambda L_4) + \\
& a\lambda^3(2(-6b(3a^5 + 2b^5) + a^2(4a^6 - 3a^5b - 5a^3b^3 + 6ab^5 - 2b^6)\lambda^2)L_1 + \\
& 6a^2b^3(a^3 + b^3)\lambda^2L_2 + a^2(-6b(3a^5 + 2b^5)\lambda^2L_5 + (-90a^3b + 60ab^3 + (4a^6 - \\
& 3a^5b - 5a^3b^3 + 6ab^5 - 2b^6)\lambda^2)L_6 + 3a(4a^5 - 5a^2b^3 + 6b^5)\lambda^2L_7 + 3a^3(3a^2b - 2b^3)\lambda^2 \\
& L_8)))(a\lambda(18 + (3a^2 - 2b^2)\lambda^2)\cosh(\lambda(a - r_0)) + (-18 + (-9a^2 + 2b^2)\lambda^2) \\
& \sinh(\lambda(a - r_0)) - \lambda(18 + b^2\lambda^2)r_0)) / ((3a^5 + 2b^5)(2aN_3\lambda \cosh(\lambda(a - r_0)) - \\
& 2N_4 \sinh(\lambda(a - r_0)) + 30b(-3a^3 + 2ab^2)\lambda r_0 + (4a^6 - 3a^5b - 5a^3b^3 + 6ab^5 - \\
& 2b^6)\lambda^3r_0)) + (5\lambda^3(aN_5\lambda \cosh(\lambda(a - r_0)) - 3N_1 \sinh(\lambda(a - r_0))) - 6(20a^6\lambda^2 - \\
& 27a^5b\lambda^2 + 2b^6\lambda^2 + 5a^3b(-18 + b^2\lambda^2))\cosh(\lambda r_0)L_3 + 6(20a^6\lambda^2 - 27a^5b\lambda^2 + \\
& 2b^6\lambda^2 + 5a^3b(-18 + b^2\lambda^2))\sinh(\lambda r_0)L_4 + 3N_2r_0 - 3\cosh(a\lambda)(180a^3L_3 + \\
& 3(a - b)^3(8a^2 + 9ab + 3b^2)\lambda^2L_3 + 180a^3(a - b)\lambda L_4 + (a - b)^4(4a^2 + 7ab + 4b^2) \\
& \lambda^3L_4)r_0)(6a\lambda(72b + (-16a^3 + 21a^2b - 2b^3)\lambda^2)r_0 + \lambda \cosh(\lambda(a - r_0))(a(a - b) \\
& (4a^2 + ab + b^2)\lambda^4(2a^3 + r_0^3) + 3\lambda^2(8a^2(a - b)^2(2a + b) + a(a - b)(4a^2 + ab + \\
& b^2)r_0 - 3(4a^3 - 3a^2b + b^3)r_0^2 + 24a(a - b)r_0^3) - 216a(a(b - r_0) + r_0(b + r_0))) - \\
& 3\sinh(\lambda(a - r_0))(72a(-b + r_0) + \lambda^4(2a^3(4a^3 - 3a^2b + b^3) + a(-4a^3 + 3a^2b + \\
& b^3)r_0^2 + (4a^3 - 3a^2b + b^3)r_0^3) + \lambda^2(16a^4 + 3b^3r_0 + 12a^3(-4b + r_0) - \\
& 9a^2r_0(b + 8r_0) + 8a(b^3 + 9br_0^2 + 3r_0^3)))) / (N(2aN_3\lambda \cosh(\lambda(a - r_0)) - \\
& 2N_4 \sinh(\lambda(a - r_0)) + 30b(-3a^3 + 2ab^2)\lambda r_0 + (4a^6 - 3a^5b - 5a^3b^3 + \\
& 6ab^5 - 2b^6)\lambda^3r_0)) \right\} \quad (\text{A16h})
\end{aligned}$$

where



$$\begin{aligned}
N = & (-12r_0\lambda(20a^6\lambda^2 - 27a^5b\lambda^2 + 2b^6\lambda^2 + 5a^3b(-18 + b^2\lambda^2)) + \\
& \lambda(-540a^3(a(b - r_0) + r_0(b + r_0)) + 3(4a(10a^6 - 21a^5b + 10a^3b^3 + b^6) + \\
& (a - b)^4(4a^2 + 7ab + 4b^2)r_0 - 3(a - b)^3(8a^2 + 9ab + 3b^2)r_0^2 + \\
& 60a^3(a - b)r_0^3)\lambda^2 + (a - b)^4(4a^2 + 7ab + 4b^2)(2a^3 + r_0^3)\lambda^4)\cosh((a - r_0)\lambda) - \\
& 3(180a^3(-b + r_0) + (40a^6 + b^5(4b - 9r_0) + 30a^2b^3r_0 + 24a^5(-6b + r_0) - \\
& 45a^4r_0(b + 4r_0) + 20a^3(2b^3 + 9br_0^2 + 3r_0^3))\lambda^2 + (a - b)^3(2a^3(8a^2 + 9ab + 3b^2) - \\
& (a - b)(4a^2 + 7ab + 4b^2)r_0^2 + (8a^2 + 9ab + 3b^2)r_0^3)\lambda^4)\sinh((a - r_0)\lambda)) \tag{A17a}
\end{aligned}$$

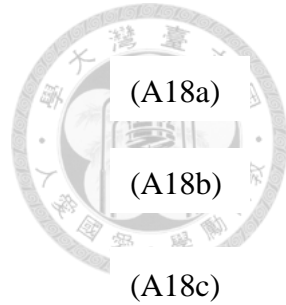
$$\begin{aligned}
N_1 = & (-180a^3bL_1 + 2(2b^6L_1 + 5a^3b^3(4L_1 + 3L_2) - 9a^5b(8L_1 + 5L_5) + \\
& 10a^6(2L_1 + 3(L_6 + L_7)))\lambda^2 + a^2(2b^6(-L_2 + L_5) - 3ab^5(2L_1 + 2L_2 + L_6 + L_7) + \\
& 4a^6(4L_1 + 2L_6 + 7L_7 - L_8) - 3a^5b(10L_1 + 14L_5 + 5L_6 + L_8) + \\
& a^3b^3(20L_1 + 14L_2 + 5(2(L_5 + L_6) + L_7) + L_8))\lambda^4) \tag{A17b}
\end{aligned}$$

$$\begin{aligned}
N_2 = & (180a^3bL_1\lambda - 2(2b^6L_1 + 5a^3b^3(L_1 + 3L_2) - 9a^5b(3L_1 + 5L_5) + \\
& 10a^6(2L_1 + 3L_7))\lambda^3 + a^2(2b^6(L_2 - L_5) + 3ab^5(-L_2 + L_7) + \\
& a^3b^3(L_2 + 5L_5 - 5L_7 - L_8) + 2a^6(L_7 - L_8) + 3a^5b(-L_5 + L_8))\lambda^5 + \\
& (180a^3L_4 + 180a^3(a - b)L_3\lambda + 3(a - b)^3(8a^2 + 9ab + 3b^2)L_4\lambda^2 + \\
& (a - b)^4(4a^2 + 7ab + 4b^2)L_3\lambda^3)\sinh(\lambda a)) \tag{A17c}
\end{aligned}$$

$$N_3 = 45a^3b - 30ab^3 + (4a^6 + 3a^5b - 10a^3b^3 + 6ab^5 - 3b^6)\lambda^2 \tag{A17d}$$

$$N_4 = 45a^3b - 30ab^3 + (4a^6 + 24a^5b - 20a^3b^3 + 6ab^5 + b^6)\lambda^2 \tag{A17e}$$

$$\begin{aligned}
N_5 = & -540a^3bL_1 + 6\lambda^2(2b^6L_1 + 5a^3b^3(4L_1 + 3L_2) - \\
& 3a^5b(14L_1 + 15L_5 + 10L_6) + 10a^6(2L_1 + 3(L_6 + L_7))) + \\
& a^2\lambda^4(2b^6(4L_1 + 3(L_2 + L_5) + 2L_6) - 9ab^5(2L_1 + 2L_2 + L_6 + L_7) \\
& + 4a^6(2L_1 + L_6 + 6L_7 - 3L_8) - 9a^5b(2L_1 + 4L_5 + L_6 - L_8) + \\
& a^3b^3(20L_1 + 12L_2 + 30L_5 + 10L_6 - 15L_7 + 3L_8)) \tag{A17f}
\end{aligned}$$



$$L_1 = \int_{r_0}^a G_{ij}(r) \mathrm{d}r \quad (\text{A18a})$$

$$L_2 = \int_a^b G_{ij}(r) \mathrm{d}r \quad (\text{A18b})$$

$$L_3 = \int_{r_0}^a \alpha(\lambda r) G_{ij}(r) \mathrm{d}r \quad (\text{A18c})$$

$$L_4 = \int_{r_0}^a \beta(\lambda r) G_{ij}(r) \mathrm{d}r \quad (\text{A18d})$$

$$L_5 = \int_a^b \left(\frac{r}{a}\right)^2 G_{ij}(r) \mathrm{d}r \quad (\text{A18e})$$

$$L_6 = \int_{r_0}^a \left(\frac{r}{a}\right)^3 G_{ij}(r) \mathrm{d}r \quad (\text{A18f})$$

$$L_7 = \int_a^b \left(\frac{r}{a}\right)^3 G_{ij}(r) \mathrm{d}r \quad (\text{A18g})$$

$$L_8 = \int_a^b \left(\frac{r}{a}\right)^5 G_{ij}(r) \mathrm{d}r \quad (\text{A18h})$$